

# Sedimentological parameterization of shallow-marine reservoirs

John A. Howell<sup>1,2</sup>, Arne Skorstad<sup>3</sup>, Alister MacDonald<sup>4</sup>, Alex Fordham<sup>2</sup>, Stephen Flint<sup>2</sup>, Bjørn Fjellvoll<sup>3</sup> and Tom Manzocchi<sup>5</sup>

<sup>1</sup>*Department of Earth Science/Centre for Integrated Petroleum Research, University of Bergen, Allegt. N-5007 Bergen, Norway*

<sup>2</sup>*Sequence Stratigraphy Group, Department of Earth and Ocean Sciences, University of Liverpool, Liverpool L69 3GP, UK*

<sup>3</sup>*Norwegian Computing Center, PO Box 114 Blindern, N-0314 Oslo, Norway*

<sup>4</sup>*Roxar Software Solutions, 165 Skoyen, Karenslyst Alle 11, 0212 Oslo, Norway*

<sup>5</sup>*Fault Analysis Group, UCD School of Geological Sciences, University College Dublin, Belfield, Dublin, Ireland*

**ABSTRACT:** The key causes of heterogeneity within progradational shallow-marine reservoirs have been defined as: shoreline type (wave vs. fluvial dominated); shoreline trajectory; the presence of permeability contrasts associated with dipping clinoform surfaces within the shoreface or delta front; the presence of cemented barriers between parasequences; and the progradation direction of the shoreline (described with respect to the main waterflood direction in the simulated reservoir). These parameters were recorded from a series of 56 modern and ancient depositional systems from a variety of climatic and tectonic settings. These data were then used to build the 408 synthetic sedimentological models that formed the basis for the SAIGUP study.

**KEYWORDS:** *shoreface, delta, reservoir, modelling*

## INTRODUCTION

Siliciclastic shallow-marine deposits form reservoirs in many of the world's major hydrocarbon provinces (e.g. North Sea, Nigeria, Brunei, Venezuela, etc.). Whilst the sedimentology and stratigraphy of such successions is well documented (for reviews see Bhattacharya & Walker 1992; Reading & Collinson 1996) little work is available publicly that quantitatively assesses controls on reservoir performance and systematically compares the production characteristics of different types of shallow-marine systems; exceptions include Ainsworth (2005), Abbots & van Kuyk (1997) and Ainsworth *et al.* (1999). The aim of the work presented here is to determine the key factors that control reservoir heterogeneity within shallow-marine systems and to outline the inclusion of these heterogeneities in models built within the framework of the SAIGUP project (Manzocchi *et al.* 2008). SAIGUP was a multi-disciplinary project aimed at quantifying the controls on hydrocarbon production from faulted, shallow-marine reservoirs. To address this, a series of synthetic sedimentological models were built. Four different structural styles were then superimposed on these and a range of different fault characteristics was applied. Subsequently, each of the models was produced using four different well patterns. The results of the flow simulations were analysed statistically to investigate the relative importance of the different input parameters and their inter-dependencies (e.g. Skorstad *et al.* 2008). The multidimensional space encompassed by the various synthetic models is termed 'SAIGUP space'. This paper documents the parameterization of the sedimentological portion of SAIGUP space and the procedures developed for building the models. A brief summary of shallow-marine systems is given and the key causes of heterogeneity within such reservoirs are discussed. Measurements of the main factors that cause

heterogeneity are presented from a variety of modern and ancient systems. These factors have then been grouped into a series of higher-order parameters that have been used to condition the 408 sedimentological models used in the SAIGUP study.

It is recognized that every depositional system and, consequently, every reservoir is essentially unique (Ainsworth *et al.* 2008). Furthermore, even the best reservoir models, built specifically for a given field, do not capture all of the subtleties of the depositional system. The challenge within this study has been to build a suite of models from a range of realistic parameters that capture the essence of progradational shallow-marine reservoirs. More detailed models of individual facies associations have not been included. The models have been used to test a whole range of parameters that affect simulated hydrocarbon production. This challenge is complicated further by the need to automate the model-building process as described below. The final suite of models is intended to represent the range of depositional systems that can occur and, while no model is a direct representation of a single shoreline system, the suite of models should capture the majority of the variability that can exist in the real world.

## SEDIMENTOLOGY OF PROGRADATIONAL SHALLOW-MARINE SYSTEMS: A BRIEF REVIEW

The shallow-marine or coastal realm is defined as the depositional system that exists between the landward influence of marine processes and the seaward influence of continental, mainly fluvial (river) processes (Boyd *et al.* 1992; Reading & Collinson 1996). The SAIGUP study concentrates on the shallow-marine and coastal realm and includes the linked depositional systems of the mud-rich inner shelf, basinward of

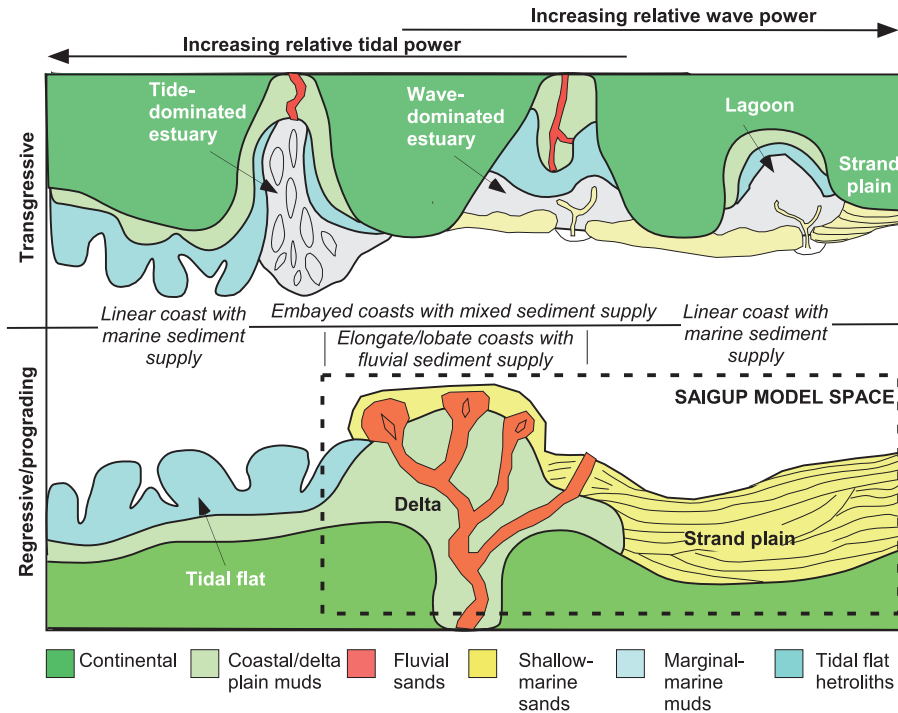


**Fig. 1.** Classification of shallow-marine shoreline systems based upon the long-term movement of the shoreline and the key depositional processes. The systems represented within the present study are enclosed in the dashed box. Modified after Boyd *et al.* (1992).

the coastal zone and the fluvial coastal/delta-plain deposits laid down landward of the shoreline.

Shallow-marine systems are classified in a number of ways. The first stage of classification is based upon medium to long-term (hundreds to tens of thousands of years) movement of the shoreline (Fig. 1). This shoreline movement is controlled by the balance between the amount of sediment supplied to the depositional system and the amount of accommodation created (Van Wagoner *et al.* 1990; Swift *et al.* 1991; Boyd *et al.* 1992). Sediment is supplied by rivers and by longshore drift, whilst accommodation is created by a combination of sea-level rise and subsidence. If the amount of sediment supplied is greater than the available accommodation then the shoreline will prograde (Van Wagoner *et al.* 1990). Modern progradational shorelines include the Mississippi delta, the Nile delta and many others (Fig. 2). Conversely, if the amount of accommodation created is greater than the amount of sediment that would be required to fill it, then the shoreline will migrate in a landward direction. Landward migration of the shoreline may occur as a result of a relative sea-level rise (tectonic or eustatic) or as a consequence of a reduction in sediment supply, such as that caused by delta lobe avulsion and auto-retreat (Van Wagoner *et al.* 1990; Muto & Steel 2001). Landward-migrating systems are termed retrogradational or transgressive and are characterized by either barrier-island complexes (such as the modern-day Texas Gulf coast) or by estuaries (such as the Thames, Severn or Dee). This study concentrates on progradational systems because they are volumetrically most significant as reservoirs (Whateley & Pickering 1989); examples include the Niger Delta (Doust & Omatsola 1990), the palaeo-Baram Delta of Borneo and Brunei (Sandal 1996; Hodgetts *et al.* 2001; Back *et al.* 2005), the Brent Delta of the North Sea (Helland-Hansen *et al.* 1992; Hampson *et al.* 2004; Jennette & Riley 1996) and many others.

The most volumetrically abundant transgressive deposits are laterally restricted estuarine systems, which are far more complex and not suited to a project such as SAIGUP. Away from estuarine settings, transgressive phases are typically represented by flooding surfaces and/or thin discontinuous shelf sand-

bodies that rarely preserve significant volumes of sediment in the shallow-marine realm and, consequently, are uncommon as reservoirs. It is important to note that certain systems, such as the Tarbert Formation of the Jurassic Brent Group in the North Sea, are described as transgressive (Hampson *et al.* 2004) because the long-term shoreline trajectory is backstepping (i.e. moving landward). However, whilst the individual shoreline parasequences (*sensu* Van Wagoner *et al.* 1990) are still progradational, it is the larger-scale parasequence set that is transgressive.

Progradational shallow-marine shorelines are subdivided further based upon the dominant depositional process. Three key processes have been identified: fluvial processes, wave processes and tidal processes (Galloway 1975; Boyd *et al.* 1992; Ainsworth *et al.* 2008). All shallow-marine systems are affected to a greater or lesser degree by all of these processes and, consequently, progradational shoreline systems are classified within a ternary scheme (Fig. 2). Any point within the triangle is defined by the relative importance of the three processes in controlling the resultant facies (and, ultimately, reservoir) architecture.

The models within SAIGUP include a spectrum from wave-dominated shorefaces through wave-influenced deltas to fluvial-dominated deltas (see Bhattacharya & Giosan (2003) for a review). The shoreface systems tend to have laterally extensive, straight strand-plain shorelines that contain few if any channels. Recent examples include the progradational parts of the modern-day coast of the Gulf of Mexico and the Nayarit Coast of Mexico (Curry *et al.* 1969; Fig. 3). Wave-influenced deltaic systems are generally lobate, sand-dominated systems with a low proportion of distributary channels, modern examples include the Sao Francisco in Brazil (Dominguez *et al.* 1987; Dominguez 1996), the Baram in Borneo (Sandal 1996), the Ebro in Spain (Somoza *et al.* 1998) and the Nile in Egypt (Sestini 1989; Hampson & Howell 2005). Fluvial-dominated deltas tend to be highly lobate to elongate, they contain abundant channels and are typically heterolithic (Bhattacharya & Giosan 2003). Modern examples include the Mississippi (Coleman & Prior 1982).

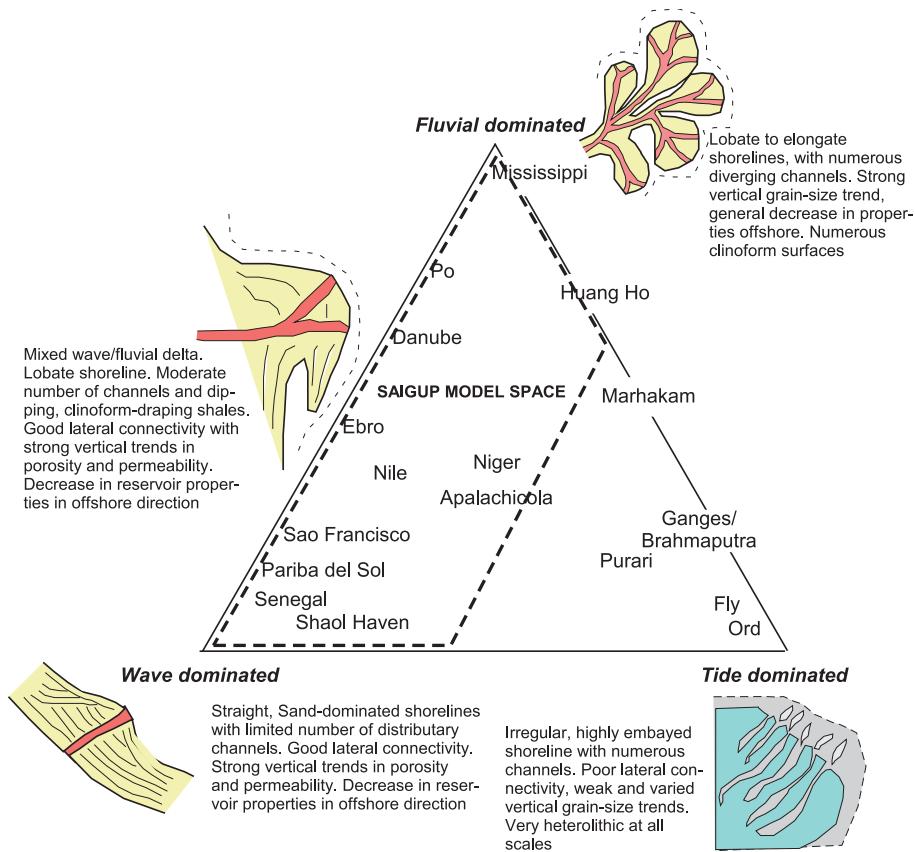


**Fig. 2.** Triangular classification of progradational shallow-marine systems based on key depositional process. Selected modern systems are indicated by name. Modified after Galloway (1975).

Whilst deltas dominated by tidal processes exist (e.g. the Modern Ganges–Brahmaputra and the Fly River; Dalrymple *et al.* 2003) and form important and extremely heterogeneous subsurface reservoir intervals, such as the Tilje and Ile formations of the Norwegian Sea (Martinius *et al.* 2005), they are rare. Tidal systems are more typically in transgressive systems, where the amplification of the tide – required to overprint the other processes – is provided by the drowning of an incised topography (Bhattacharya & Walker 1992; Zaitlin *et al.* 1994). Consequently, they are not considered further within this study.

#### Sedimentological controls on reservoir architecture within shorefaces and wave-dominated delta systems

In wave-dominated, shallow-marine depositional systems, the majority of sediment is brought to the shoreline by fluvial systems, although locally significant amounts may also be sourced from wave erosion of older sediment along the coast (Fig. 3). The sediment is transported along the shoreline by longshore drift until it is deposited (Reading & Collinson 1996; Bhattacharya & Giosan 2003; Howell 2005). The top of the depositional system (the delta or coastal plain) is essentially flat (typical dips of  $<0.02^\circ$ ) and sits just above mean sea-level on the landward side of the shoreline. On the seaward side of the shoreline the shoreface is defined as the interval between the mean sea-level and the mean fair-weather wave base (FWWB, Walker & Plint 1992). FWWB is the depth to which the typical daily waves affect the sea bottom. Seaward of the shoreface and extending to mean storm wave base (SWB) is the offshore transition zone (OTZ) and, further seaward still, is the offshore (Fig. 3).

Immediately behind the shoreline are a series of lagoons and a low-lying coastal plain. The majority of sand in the coastal plain is deposited by fluvial systems, although beach ridges may

exist immediately behind the shoreline (Dominguez *et al.* 1987). Channels, which are frequently meandering due to their low gradient, deposit sand in narrow channel belts. Outside the channel belt, overbank deposits are laid down. These overbank deposits are comprised mainly of mudstones, although thin sandstones and coals may also be present (Ryer 1981; Howell & Flint 2004). The overbank deposits are laid down either under subaqueous conditions in lagoons, or on floodplains that are generally subaerial. Processes on the floodplain include sheet-floods and deposition of fine material from suspension in ephemeral ponds and lakes. The channel sandbodies will generally have good reservoir properties, although their lateral extent is typically limited. The overbank deposits are effectively non-reservoir, although in some cases crevasse splay systems can contribute to net reservoir pay (Keogh *et al.* 2005).

Sediment introduced to the marine part of the system is transported along the shoreface by longshore transport processes, whilst fair-weather waves steadily move the sediment obliquely landward and deposit a series of trough cross-bedded (TXS) sandstones in the upper shoreface (USF), which are overlain by planar-laminated sandstones deposited by the swash from the breaking waves on the foreshore. These deposits are typically very mineralogically and texturally mature, have a very low clay content and generally make excellent reservoirs, such as the Etive and Tarbet formations in the Brent Group (Hampson *et al.* 2004).

Periodic storms erode the upper shoreface and foreshore and deposit sheets of hummocky cross-stratified sandstones across the lower shoreface and OTZ. During fair-weather periods, the waves rework the tops of hummocky cross-stratified beds in the lower shoreface but do not affect those in the OTZ. Fair-weather deposition in the OTZ is characterized by silt and mud deposited from suspension. The hummocky

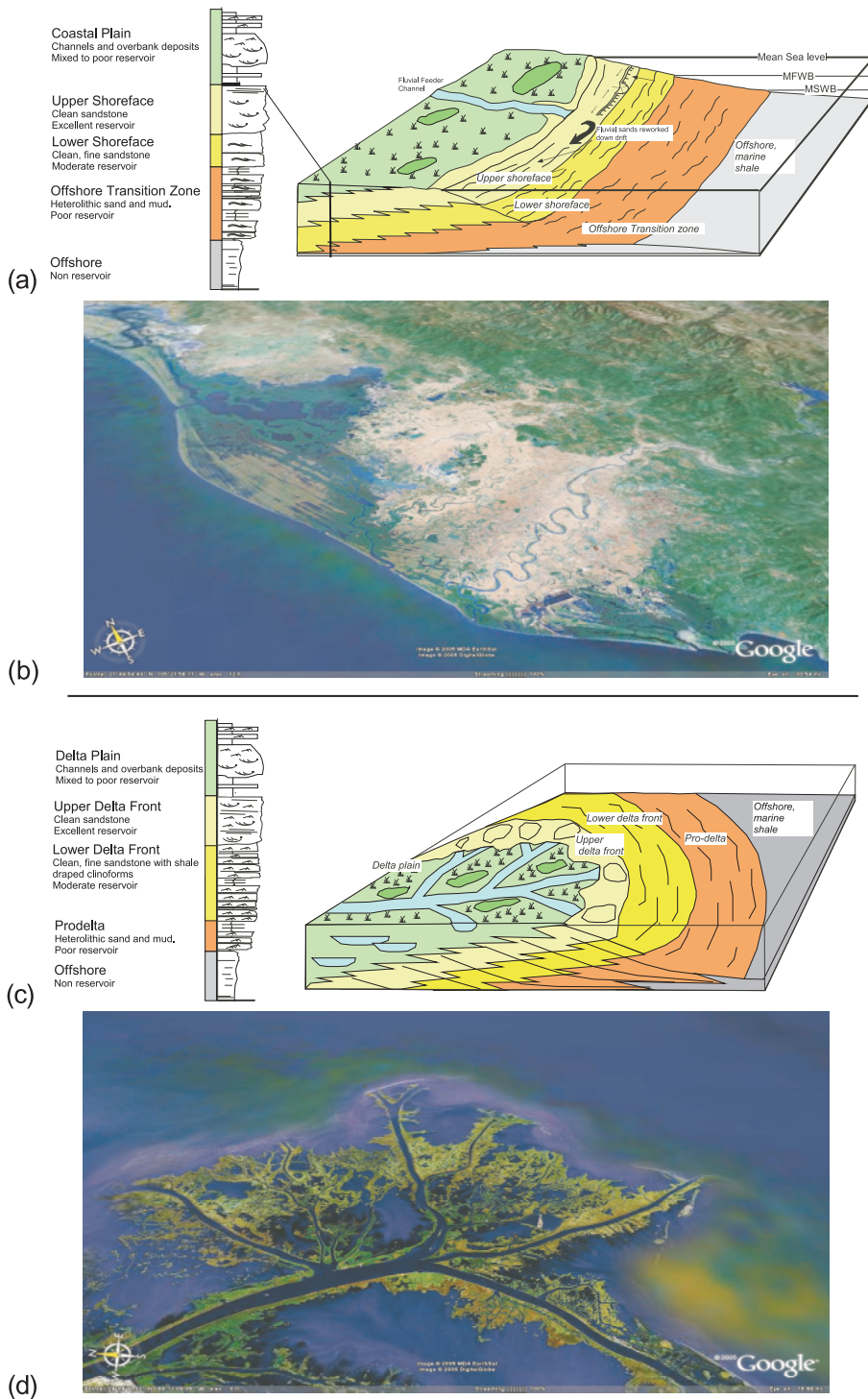


**Fig. 3.** Facies models for shoreface and deltaic systems highlighting the terminology used in this work. (a) Depositional model for a shoreface and wave-dominated delta. MFWB, mean fair-weather wave base; MSWB, mean storm wave base. (b) Oblique satellite view of the Nayarit Coast, Mexico, a modern wave-dominated shoreline (Google Earth 2007; field of view is  $\approx$  30 km wide). The view includes shorefaces and wave-dominated deltas. (c) Depositional model for a fluvial-dominated delta. (d) Oblique satellite view of the Balize lobe of the Mississippi, a modern river-dominated delta (Google Earth 2007; field of view is  $\approx$  30 km wide).

cross-stratified beds are generally finer grained than those of the upper shoreface, and the lower shoreface interval may contain thin, discontinuous mudstone horizons. Consequently, the reservoir properties are poorer than the upper shoreface. In many cases, such as the Fulmar Formation in the Central North Sea, the lower shoreface may also become extensively bioturbated (Howell *et al.* 1996). The lower shoreface interval is still sand dominated and will typically contribute to hydrocarbon production. The hummocky cross-stratified beds in the OTZ have similar reservoir properties to those in the lower shoreface, but the beds occur as laterally extensive sheets separated by mudstones. Consequently, whilst horizontal flow

properties may be good, vertical flow between beds is very limited. Beds in the OTZ will connect up depositional-dip to those in the lower shoreface, where better vertical communication exists. Seaward of the OTZ and below SWB, deposition is of hemipelagic and pelagic silt and clay. Whilst it is noted that storm-derived density currents can carry sand-grade sediment far offshore (Pattison 2005), these events appear to be relatively rare in the rock record and the offshore deposits are treated as non-reservoir.

Consequently, a typical succession (Fig. 3) passes up from offshore mudstones through interbedded, hummocky cross-stratified sandstone and mudstone into the sandstones of the

shoreface. The lower part of the shoreface is characterized by amalgamated hummocky beds, while the upper part is characterized by trough cross- and planar bedding. This is overlain by the channel and overbank deposits of the coastal plain. Overall, there is an upward increase in reservoir properties up to the top of the foreshore, while the coastal plain is highly variable.

In a depositional dip direction (i.e. a profile from onshore to offshore), the top of the delta plain is essentially flat, the shoreface and OTZ exhibit a dip, typically of 1–2° that decreases into the offshore (Hampson & Storms 2003; Hampson & Howell 2005). In a depositional strike direction (i.e. along the shoreline), wave-dominated deltas are generally straight to slightly lobate (Fig. 3).

### Sedimentological controls on reservoir properties and architecture within river-dominated delta systems

Within river-dominated delta systems, the sediment brought in by the fluvial system is not redistributed by either wave or tide processes. As the sediment-laden river enters the standing body of water, the flow decelerates and causes deposition of the load. The basic depositional element in a river-dominated delta is the mouth bar (Coleman & Prior 1982; Reading & Collinson 1996). As the mouth bar aggrades it eventually becomes emergent and diverges the river into two distributary channels on either side of the bar. Two smaller mouth bars are then deposited in the mouths of these channels and the channels continue to split until they become too small to carry sediment. The system becomes choked and avulsion or lobe switching occurs (Olariu & Bhattacharya 2006), where the river breaks from its existing channel and establishes a new lobe in a topographically lower area, typically in a lateral position to the existing lobe. River-dominated delta lobes are highly lobate to finger-like in geometry and contain abundant channels (Fig. 3).

At the front of the delta, the finest sediment is carried furthest into the basin in a buoyant plume and the coarsest material is deposited nearest to the river mouth. Periodic floods in the river release sediment that is flushed into the delta system. Each flood results in a sheet of sandstone that dips, thins and fines in a seaward direction. These are termed clinofolds (Driscoll & Karner 1999). The sheets are dominated typically by planar laminations and ripple cross-lamination. In the lower delta front (pro-delta), thin sheets of sandstone – representing the seaward extent of the largest floods – are interbedded with the mudstones deposited from suspension through much of the time. The middle and upper parts of the delta front (LDF and UDF) contain a progressively higher proportion of sand in thicker beds. The UDF may be cut by and interfinger with the deposits of the distributary channel (Anderson *et al.* 2004). Landward of the shoreline lies the delta plain, which, like the coastal plain described above, is comprised of channels and overbank deposits (Ryer 1981; Reading & Collinson 1996). Typically, there is a greater proportion of channel deposits in the delta plain than in wave-dominated coastal plain because the number of active channels at any one time is greater.

Because the sediment is not significantly reworked by waves, river-dominated deltas are highly lobate (e.g. Newman & Chan 1991; Anderson *et al.* 2004; Bhattacharya & Tye 2004). The mouth-bar sandbodies also contain seaward-dipping clinofold surfaces (e.g. Ryer & Anderson 2004). These clinofolds represent former positions of the depositional surface that existed between flood-induced influxes of sand. They dip in a seaward direction and frequently are draped with mud. These mud-draped surfaces are potential significant barriers to both

horizontal and vertical fluid flow within mouth-bar reservoirs (Driscoll & Karner 1999).

### Parasequences and parasequence sets

Parasequences are the basic building blocks of sequence stratigraphy (Van Wagoner *et al.* 1990) and the parasequence concept has been used as a stratigraphic framework for the models in the SAIGUP study. Within a deltaic or shoreface parasequence there is an upward increase in grain size and sandstone-bed thickness and a decrease in the proportion of shale, all of which result from the reduction in depositional water depth as the shoreline system progrades (Van Wagoner *et al.* 1990). Parasequences are bounded by flooding surfaces where there is a sharp increase in the amount of shale, resulting from a landward dislocation of facies associated with a rapid rise in relative sea-level. These flooding surfaces are typically the key tools for correlation within shallow-marine reservoirs.

Parasequences stack into parasequence sets, which are defined as a set of genetically related parasequences with a consistent stacking pattern (Van Wagoner *et al.* 1990). The stacking pattern records the longer-term movement of the shoreline during the deposition of a number of parasequences. Parasequence sets may be progradational, aggradational or retrogradational, depending upon whether the shoreline is moving seaward, landward or remaining stationary through time. The main suite of synthetic reservoir models in SAIGUP is comprised of four equally thick (20 m) parasequences, stacked in a progradational parasequence set. The justification for this is discussed further below.

## DATA COLLECTION AND MODEL PARAMETERIZATION

Shorefaces and river-dominated deltas are two end-members of a spectrum of delta types (Fig. 2). There are broad similarities in that both types of deposit coarsen upward from offshore mudstones, through a variety of heterolithic and sand-rich deposits and are overlain by coastal plain deposits. However, significant differences exist both between the plan view geometries of these systems and their internal character. The aim of this study is to quantify a series of parameters that define these differences and to populate the SAIGUP models with realistic values. For this purpose data were compiled from a series of 15 ancient and 41 modern shoreline systems (Tables 1 and 2). The data were taken from published work, including cross-sections and maps for ancient systems and from maps, satellite and aerial photographs of modern systems. Extensive use was made of NASA's 'Earth from Space' (NASA 2003) and MrSid Landsat database (NASA 2004).

The key parameters, which are outlined below, were subdivided into two groups: (1) those that were varied within model building in order to introduce the required heterogeneities to the synthetic reservoirs; and (2) those that were treated as constant across the full suite of models. Many of these parameters have a degree of interdependence; this was investigated and included in the model parameterization.

It is recognized that the modern-day shape of a delta represents a 'snap-shot' of the processes and forms that result in the final preserved depositional element. The final depositional element will commonly be larger and more extensive than the present-day view. However, the majority of these features, such as delta lobes and shorefaces, are preserved by rapid abandonment and flooding during the formation of a parasequence boundary. This process results in the 'fossilization' of the form that was present immediately prior to the

**Table 1.** Key parameters for selected ancient progradational shoreline systems

System	Time			Distance		Climoforms			Facies thickness				Lithology	
	Age (Ma)	Duration (Ma)	Subsidence rate (mm ka <sup>-1</sup> )	Progradation distance (m)	Element displacement (m)	Aggradation angle (°)	Climoform spacing (m)	Climoform dip (°)	Coastal plain thickness (m)	Upper shoreface thickness (m)	Lower shoreface thickness (m)	Transition zone thickness (m)		Offshore thickness (m)
Panther Tongue, Book Cliffs, USA	80.5	0.5	10	15850	700	0.07	8.18	2.1	0	8.32	19.1	5.35		6
Spring Canyon Mb, Book Cliffs, USA	82.0	0.5	20	4628	2240	0.21	1100	0.27	4.20	6.56	9.93	5.57		5.00
Kenilworth Mb, Book Cliffs, USA	81.5	0.5	20	18783	5014	0.04	30	0.04		5.62	4.11	22.30		7.00
Sunnyside Mb, Book Cliffs, USA	81.0	0.5	20	12287		0.10	2010	0.22		4.30	13.47	8.33		6.00
Grassy Mb, Book Cliffs, USA	80.0	0.5	20	12766	4291	0.13	3100	0.06		8.33	12.44	9.26	27.00	6.00
Ferron Sst, Wasatch Plat, USA	85.0	0.8	35	10500	3000	1.90	3.2	5.2		5.70	14.20	12.00		6.00
Ferron Sst, Wasatch Plat, USA	86.0	0.8	35	12200	2600	1.10	8.3	6.4		6.90	11.70	14.00		6.00
John Henry Mb, Kaiparowits Plateau, USA	88.0	1	30							39.80	29.08	2.73	3.00	6.00
Judith River Fm, Big Horn Basin, USA	80.0	4	30							5.80	7.80	3.90	10.00	6.00
Mesaverde, northwestern Colorado, USA	82.0	6.5	35							10.00	5.78			6.00
The Clyde Field, North Sea Central Graben	156.0	1	120							6.45	8.70	11.23		7.00
The Cormorant Field, East Shetland Basin	219.0	1.5	5							3.52	12.50	11.70		7.00
Thistle Field, North Viking Graben	168.0	3	5							6.45	15.85	7.40		7.00
The Hutton Field, East Shetland Basin	168.0	3	5							6.45	5.60	4.84		7.00
The Tern Field, East Shetland Basin	168.0	3	5							1.54	2.05			7.00

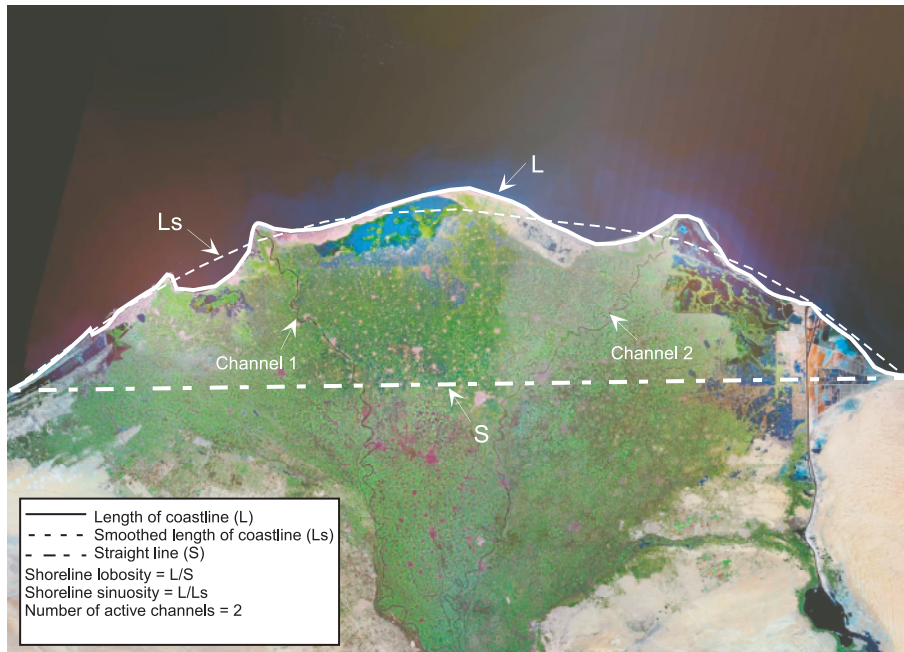
<sup>a</sup>Type of delta according to grain size (GR, Gravel; GS, gravel and sand; FS, fine sand; MS, mud/silt) and dominant processes shaping delta front (i, input dominated; t, tide dominated; w, wave dominated; m, mixed).

Table 2. Key parameters from modern progradational shoreline systems

Delta	Delta plain					Delta slope			Basin regime			
	Type <sup>a</sup>	Drainage area (10 <sup>3</sup> km <sup>2</sup> )	Mean grain size (mm)	Area (km <sup>2</sup> )	Delta front lobosity	Shoreline sinuosity	Channel mouths (no.)	Channel sinuosity	Upper delta slope gradient (mean or range; m km <sup>-1</sup> )	Mean slope angle (°)	Mean tidal range (m)	Mean water depth (m)
Alta	GSt		10						90–700	23.30	1–2.5	70
Amazon	MSit	6 150.0	0.03	467 078					1.0–10.0	0.29	4.9	100
Bella Coola	GStw	4.2	10.25	5					73–268	9.79	3.9	600
Burdakin	FS/GSm	266.7	0.75	2 112	1.22	2.20	1	1.25			2.2	
Chachgula	GRw	0.07	2	6					40	2.29	low	
Colville	GS	59.5	5.01	1 687	1.64	2.04	5	1.08			0.2	
Copper	FSwt	60	0.25	1 920					3.0–11.0	0.40	3.4	150
Danube		712.6		2 740	1.39	1.22	5	1.38				
Dneiper		801.3										
Ebro	FSwi	85.8	0.2	325	2.07	2.14	12	1.12	8.7	0.50	0.2	100
Fraser	FSit	234	0.24	480					25	1.43	5	350
Ganges/Bramaputra		1 597.2	0.16	105 641	1.03	3.67	20	1.08	0.18	0.01	3.6	
Homanthko	GSt	5.72	0.14	3	1.01	1.00	5	1.09	20–110	3.73	4	550
Huanghe	MSi	865.1	0.04	36 272	1.13	2.23	5	1.16	6	0.34	0.8	30–50
Irrawaddy	MSm	341.8	0.02	20 571	1.16	3.64	13	1.25	0.6	0.034	4.2	<100
Jaba	GS <sup>w</sup>	0.46		4							1.5	
Klang	FSt	0.9	0.16	1 817							0.2	
Klimaklini	GSt	6.5	0.5	6					20–80	2.87	3.6	350
Mackenzie	FSi	1 448.0	0.062	13 000	1.39	2.34	14	1.30	0.29	0.017	0.2	870
Mahakam	FSit			5 000	1.35	4.6	5	1.38	65	3.73	1.2	100
Mekong	Fsm	790.0	0.10	93 781	1.04	1.78	7	1.07	0.5	0.029	2.6	
Mississippi	MSi	3 344	0.014	28 568	5.25	2.46	17	1.09	3.0–15.0	0.5	0.4	
Niger	Fsm	1 112.7	0.15	19 135	1.19	1.00	13	1.74	2	0.11	1.4	100–200
Nile	FSwi	2 715.6	0.03	12 512	1.09	1.18	6	1.50	0.265	0.015	0.4	100
Noeick	GSt	0.562		0.8					80–110	5.45		250
Ord	MSt	78.0	0.176	3 896							3.8	
Orinoco	Msm	951.3		20 642	1.11	1.76	37	1.53	0.45	0.026	1.9	
Po	FSi	71.7	0.52	13 398	1.33	2.13	9	1.28	3.3	0.19	0.7	
Punta Gorda	GRw	0.005	225	0.4	1.06	1.00	2	1.25	40	2.29		
Rhone	FSwi	90.0	0.29	2 540	1.28	1.70	2	1.22	3.4	0.19		50–100
Sao Francisco	FSw	602.3		734	1.20	1.00	1	1.10	4.3	0.25	2.5	
Senegal	FSw	196.4		4 254	1.01	1.00	1	1.25	7	0.40	1.9	
Shoalhaven	Fsm	7.25	0.25	85					14	0.80	1.2	
Skeirdar Sandur	GSw		0.49	600	1.00	1.00	4	1.00	16	0.92	2	
Tiber	FSw	17.156	0.062	250	1.17	1.00	1	1.51	04.0–20.1	0.69		150
Tunsberg Dalbre	GRI	0.136	4.06	25					100	5.74		
Yallahs	GRwi	0.163	42	10.5	1.22	1.00	1	1.03	180	10.36	0.2	1100
Yangtze	MSit	1 354.4	0.02	66 669							2.8	50

Expanded from work presented by Orton &amp; Reading (1993).

<sup>a</sup>Type of delta according to grain size (GR, Gravel; GS, gravel and sand; FS, fine sand; MS, mud/silt) and dominant processes shaping delta front (f, input dominated; t, tide dominated; w, wave dominated; m, mixed).



**Fig. 4.** Satellite view of the modern Nile illustrating the key parameters associated with shoreline shape, recorded from modern delta systems within the study. Lobosity and number of channels are used as variable inputs to models, sinuosity is used to condition the interfingering factor. Field of view is 120 km wide (image from NASA 2004).

flooding, such that the modern systems can be used as an approximation for the facies distributions and geometries within a single parasequence. Given the limited amounts of usable data on preserved 3D architecture from ancient systems, the modern ones have been considered a usable proxy that contributes much value to the dataset.

#### Parameters varied within SAIGUP space

The type of shoreline system (see above) is traditionally considered to be the key control on the subsequent reservoir heterogeneity (Galloway 1975; Coleman & Prior 1982 and others). As discussed previously, the principal depositional process acting at the shoreline (wave vs. fluvial) controls the plan-view shape, the channel abundance in the delta plain and the abundance of mudstone-draped clinoform surfaces within the delta front. These parameters were characterized from the modern and ancient systems separately and then combined to produce a lower-order parameter, termed 'shoreline type', which was varied at three different levels within the SAIGUP modelling. These levels can be summarized as 'shorefaces', with a straight plan-view shape, very few channels and no dipping barriers; 'wave-dominated deltas', with a lobate shape, moderate numbers of channels and some dipping barriers; and 'river-dominated deltas', with an elongate shape, abundant channels and abundant dipping barriers. The detail of recorded and modelled values is discussed below, as are the other parameters (aggradation angle, barrier coverage and progradational direction) recorded and varied in the modelling.

*Shoreline shape* The plan-view shape of the shoreline is termed here the shoreline 'lobosity'. Lobosity was measured from the modern systems as the ratio between the curved profile of the delta and a straight line between a point at either side (Fig. 4). Lobosity in nature ranges as a continuous parameter from straight, through lobate to elongate (Fig. 5). Observed values from modern systems occurred in the range of 1–5.5, with a mean of 1.4. Values were not recorded from ancient systems because of the lack of reliable map view data available for most systems.

The shorelines were modelled using a truncated Gaussian simulation method (MacDonald & Aasen 1994). Using this

approach a boundary between adjacent belts of facies is modelled as a linear expectation surface, which defines the mean position of the boundary with stochastic variability subsequently added. In plan view the expectation surface can be defined as either straight or simply curved. The degree of curvature is a user-defined parameter conditioned from the measurements of the modern systems. Within SAIGUP the curvature of the shoreline was modelled at three levels of lobosity: 1.1, 1.8 and 2.9 (RMS values of 2.0, 0.6, 0.35, respectively; Fig. 5). The 1.1 value is considered to represent a near-linear shoreline, typical of wave-dominated shoreface systems; 1.8 is a moderately lobate system, typical of wave-dominated deltas; 2.9 is a highly lobate system, representative of a river-dominated delta (Fig. 5).

In the set of models containing highly lobate shorelines (lobosity of 2.9), the proportion of the zone occupied by shallow-marine facies was very low. Consequently, each zone was populated with two rather than one lobe. This was considered to be more geologically realistic as a single delta lobe sitting in isolation is unlikely to occur in nature because the space between the finger-like lobes is occupied during the next lobe avulsion event (Reading & Collinson 1996).

As mentioned previously, shoreline shape is a subset of the parameter 'shoreline type' and, as such, is also linked to clinoform abundance, clinoform geometry and channel abundance (Fig. 6). Figure 7 illustrates three SAIGUP models with real-world shallow-marine systems. Although only qualitative, the favourable comparison between model and nature is a

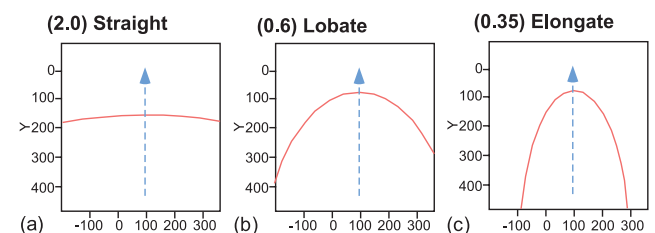


**Fig. 5.** Three levels of shoreline shapes used to build the synthetic models, as seen in RMS modelling software. Numbers refer to the RMS internal value.

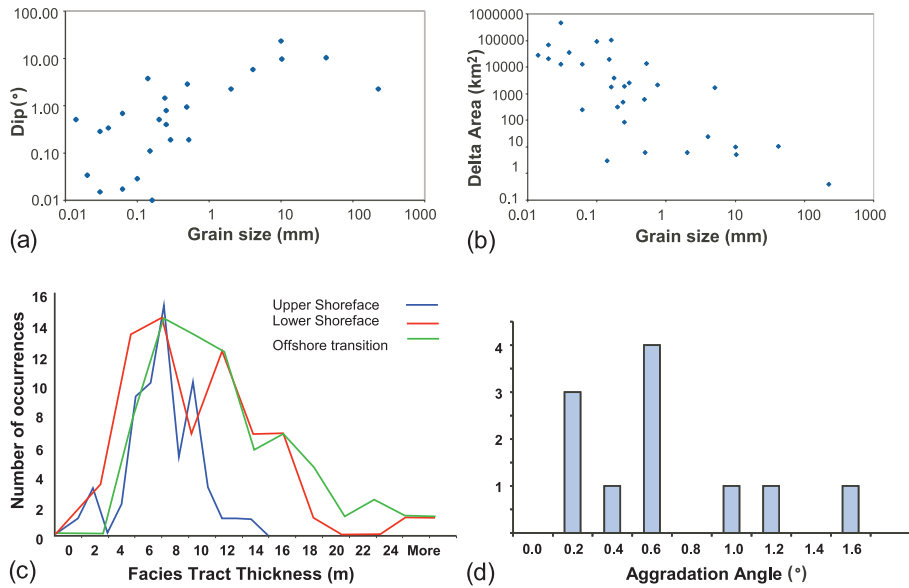


**Fig. 6.** Selected data from the compiled database illustrating: (a) the relationship between grain size and delta-front/clinoform dip; (b) grain size, delta and delta-top area; (c) frequency distribution plot showing facies tract thicknesses; (d) frequency distribution plot of measured aggradation angle (also known as shoreline trajectory).

useful quality control on the effectiveness of SAIGUP parameters at capturing real-world geometries.

**Abundance of shale-draped clinoform surfaces** Seaward-dipping clinoform surfaces are an integral part of shallow-marine systems (Driscoll & Karner 1999; Hampson 2000; Hampson & Storms 2003; Ryer & Anderson 2004). Where these surfaces are commonly draped with shale, they may provide both horizontal and vertical barriers to fluid flow (Li & White 2003; Skorstad *et al.* 2008). Such draping is most common in fluvial-dominated or fluvially influenced systems. Seaward-dipping surfaces, clinoforms, occur at a variety of scales, two of which are relevant here – the bed and the bedset (*sensu* Van Wagoner *et al.* 1990). Bed-scale clinoforms are comprised of seaward-dipping sandstone beds locally draped with thin beds of shale (Figs 3 & 8). These are especially common within river-dominated delta systems and are the product of very short-term fluctuations in the output of the feeder systems. Specific studies to address the effects of this scale of clinoform on production have been undertaken (Ainsworth *et al.* 1999; Chidsey *et al.* 2004; Skorstad *et al.* 2008). Clinoforms also exist at the larger, bedset scale in both fluvial- and wave-dominated shorelines. Individual bedsets represent lobes of the delta, the dipping front surface of which is commonly draped with significant shales, deposited when the lobes are abandoned during avulsion. Bedset-scale clinoforms have been recognized in shoreface systems (O’Byrne & Flint 1995; Pattison 1995; Hampson 2000; Howell & Flint 2004; Sømme *et al.* 2008) but are significantly more common and more potentially detrimental to fluid flow in river-dominated systems (Anderson *et al.* 2004; Skorstad *et al.* 2008). Neither bed clinoforms nor bedset clinoforms are recognized commonly in subsurface datasets and they are rarely included in reservoir models (see Ainsworth *et al.* 1999; Chidsey *et al.* 2004). Within the limited outcrop datasets available there is a clear link between clinoform abundance and shoreline shape. River-dominated systems have a far greater abundance of shale-draped clinoforms than their wave-dominated counterparts. Observations from outcrops, such as the Panther Tongue (Newman & Chan 1991; Howell *et al.* 2008; Fig. 8) and Ferron deltas in Utah (Anderson *et al.* 2004), indicate that the shape of the clinoform surfaces broadly follows the shape of the shoreline. Straight shorelines typically have planar seaward-dipping clinoforms and curved shorelines have clinoforms that resemble top-truncated cones (see below; Fig. 8).

For the purpose of SAIGUP, the bedset-scale clinoforms were modelled as stepped transmissibility multipliers on the cell faces (see below). Two factors were varied, the spacing of the clinoforms and the degree of shale coverage on the clinoform surface. It was not possible to represent accurately the closely spaced bed-scale clinoforms within a regular grid with the resolution of the SAIGUP model (or a typical field model). A separate study was initiated to investigate their effect.

As in the real world, the abundance of dipping barriers associated with clinoforms was linked to the shoreline shape. Dipping barriers were not included in the linear shoreline (shoreface) models. In the lobate shoreline (wave-dominated deltas) between one and three barriers were included, with a spacing of between 1000 m and 1500 m. A similar spacing was used for the river-dominated deltas (elongate shorelines) but there was no limit on the maximum number. Furthermore, in the river-dominated delta models, dipping barriers were placed independently in both ‘lobes’.

The degree of barrier coverage (i.e. what proportion of the barrier is represented by reduced permeability vs. what proportion is comprised of ‘holes’; see Manzocchi *et al.* 2008, fig 4 for example) was modelled independently. No real data were available from outcrop studies and values of 10%, 50% and 90% were chosen to cover a full range of possibilities. Details of the barrier modelling process are outlined below.

**Channel abundance and pattern** In natural systems, channels within the coastal plain carry the sediment to the shoreline where it undergoes variable amounts of reworking before being deposited in the shoreface or delta front. Some of that sand is deposited within the channels and ultimately contributes to the net pay and flow characteristics of the reservoir. Delta-top and coastal plain channels are commonly straight to moderately sinuous (eg Van den Bergh & Garrison 2004; Figs 3, 4 & 7). In the linear shoreline systems, either channels are absent as the sediment is supplied along the coastline by longshore drift or only a single channel is present, approximately normal to the shoreline. In delta systems the channels bifurcate downdip to form a broadly radial pattern. The channel abundance was recorded as the number of channel’s mouths at the shoreline within the modern studied systems. It was not possible to determine reliably the volume of channel facies in ancient systems as the quality of the outcrop is typically insufficient. Observations from both the modern and ancient systems

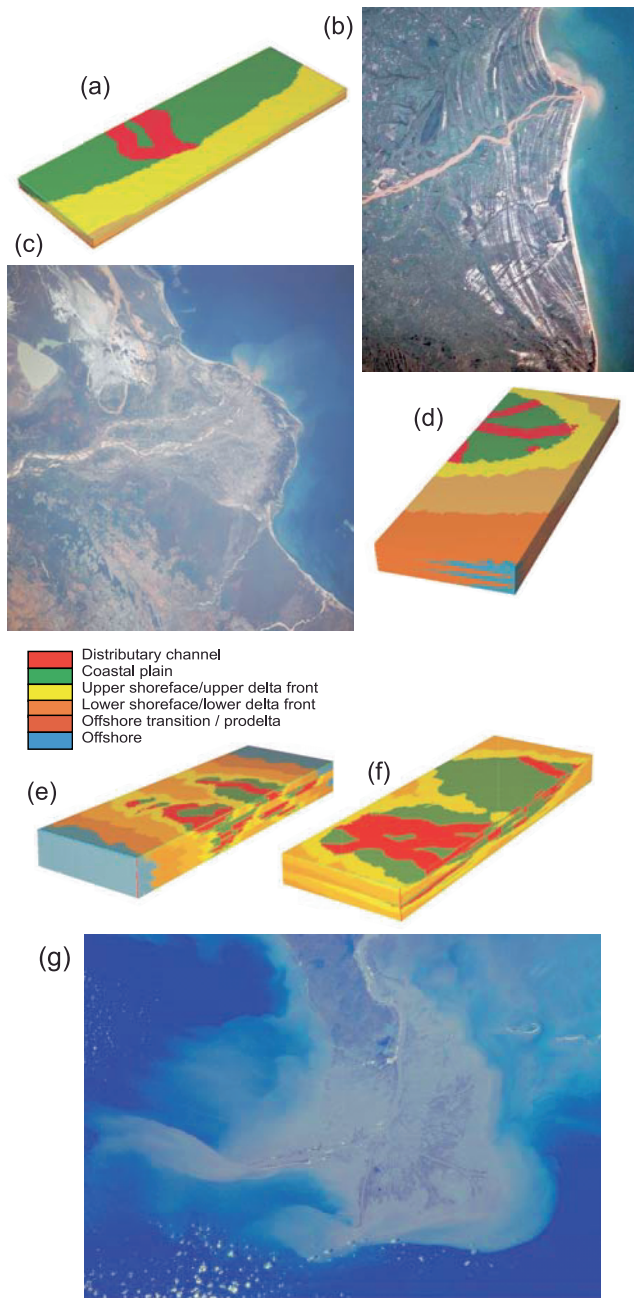


**Fig. 7.** Comparison of synthetic models with selected modern systems. (a) Model with a straight shoreline and moderate aggradation angle; model is  $9 \times 3 \times 0.08$  km. (b) Modern wave-dominated delta/shoreface from the Paraíba del Sol, Brazil; field of view is  $\approx 30$  km wide (NASA 2003). (c) Model with a lobate shoreline geometry and moderate aggradation angle. Note the radiating channel geometry; model is  $9 \times 3 \times 0.08$  km. (d) Modern mixed wave- and river-dominated delta, Mangoky River Delta, Madagascar; field of view is  $\approx 50$  km wide (NASA 2003). (e, f) Models of elongate, river-dominated deltas, each containing two lobes and built with a high (e) and low (f) aggradation angle. Both models are  $9 \times 3 \times 0.08$  km. (g) Modern river-dominated delta, the Mississippi Delta, USA; field of view  $\approx 50$  km wide (NASA 2003). Key is for the facies in the models.

indicate that the frequency and pattern of the channels within the coastal plain are related strongly to the shoreline shape (Tables 1 and 2) and are a function of the type of delta system. As a general rule, straight shorelines have a very low abundance of channels whilst more curved systems contain a greater abundance.

The main facies modelling was undertaken using parallel belts of facies. This method is highly suited to shoreface and deltaic deposits but does not capture channels as discrete objects. Therefore, the channels were modelled separately using specific channel modelling tools (see Holden *et al.* (1998) for review of method) and then merged into the coastal plain facies belt. The dimensions of the channel objects were drawn from normal distributions, such that the mean width was 500 m (standard deviation of 100 m) and the mean thickness was 10 m (standard deviation of 2 m). A moderate correlation coefficient between width and thickness was included so that wider channels tended to be thicker. The channels have infinite length within the models. The channel pattern was linked to the shoreline type, with the straight shorelines being associated with simple, broadly shore-normal channels and a point-sourced, radial channel distribution being used for the deltaic systems (Fig. 7). In merging the channels and the facies: belts model, the channel objects were placed only in the coastal plain belt. This meant that the channels provide a potentially high-permeability flow pathway through the coastal plain mudstones that is in lateral and vertical communication with the highly permeable upper shoreface/upper delta-front deposits. This is a reasonable compromise for the purpose of modelling in an automated system; however, it should be noted that in nature the channels may interfinger and even cut through older delta-front deposits, especially in systems with a low aggradation angle.

The proportion of the channels is set in the initial model, but it is somewhat difficult to control fully the proportion of channels in the final models as the channel bodies in the channel modelling stage may not be distributed uniformly in the volume so that the resampled volume does not reflect fully the original or target proportions. Therefore it is more useful to report the channel proportions in the finished models, after the resampling. The mean and standard deviation of these are  $15 \pm 2\%$ ,  $28 \pm 6\%$  and  $52 \pm 18\%$  for the straight (shoreface), curved (wave-dominated deltas) and elongate (river-dominated deltas) shorelines, respectively. All three distributions are close to normally distributed.

**Aggradation angle ( $\alpha$ )** The aggradation angle ( $\alpha$ ) or shoreline trajectory (Helland-Hansen & Martinsen 1996) records the movement of the shoreline in a 2D, depositional dip-orientated cross-section. In aggradational and progradational systems, such as those within the SAIGUP study, the trajectory may theoretically vary between simple, horizontal progradation (no climb,  $0^\circ$ ) and pure vertical aggradation ( $90^\circ$ ). Shoreline trajectory is a function of the balance between sediment supply and the rate of accommodation creation. A low  $\alpha$  occurs when the rate of sediment supply is high compared to the rate of accommodation creation and a high  $\alpha$  occurs when accommodation creation is higher and sediment supply lower. It should be noted that, as previously stated, in the studied progradation systems, the sediment supplied is always greater than the space created. It is possible to consider the shoreline trajectory over a number of different time-scales, two of which are relevant to this study: the parasequence (SAIGUP model zone) and parasequence set (entire SAIGUP reservoir). At both scales a low  $\alpha$  will result in thinner, but more laterally extensive facies tracts, while a high  $\alpha$  will result in vertical stacking of narrower facies belts (Fig. 9).

Whilst the shoreline trajectory is a useful abstract concept, measuring values from the real world is more difficult, primarily because of the variety of datum surfaces used as palaeo-horizontal in cross-sections. Shorelines with both horizontal trajectories (e.g. Hampson *et al.* 2004; Howell & Flint 2004) and

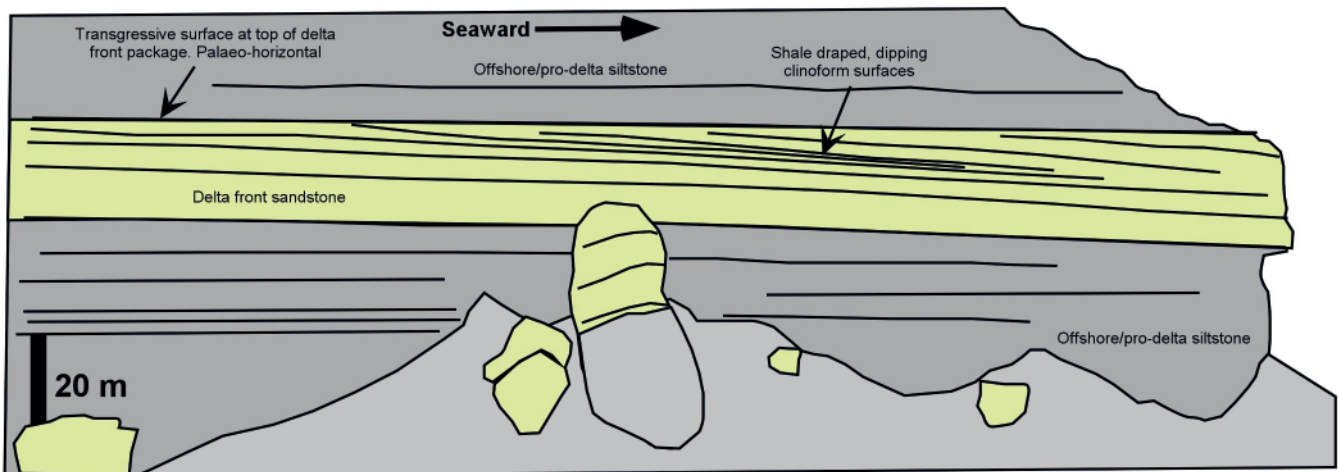


Fig. 8. Dipping clinoform surfaces within the river-dominated delta deposits of the Cretaceous Panther Tongue Sandstone in the northern Book Cliffs, Utah. Note the seaward dip of the darker, mud-draped clinoform surfaces.

climbing shoreline trajectories (e.g. Ryer 1981) have been documented from numerous outcrop studies; however, it is very difficult to quantify the actual amount of shoreline climb.

The facies tract thickness in a shoreline with a horizontal trajectory will be equivalent to the depths to mean SWB and FWB. If the shoreline is climbing (positive trajectory, aggradational) then the facies tracts will become thicker ( $\tan(\alpha)$  times the progradation distance). Typical progradational distances for shoreline may vary from hundreds of metres to tens of kilometres (Kamola & Huntoon 1995; Howell & Flint 2004). Using a conservative value, equivalent to half the length of the SAIGUP field (4 km), it can be seen that very low angles produce extremely thick shoreline units (Fig. 9b). Observed thickness values for individual shoreface packages in the rock record are between 10 m (e.g. O'Byrne & Flint 1995; Fitzsimmons & Johnson 2000) and 100 m (e.g. Johnson *et al.* 1986; Howell *et al.* 1996). These extreme values were used to define three levels of aggradation angle to be used in the modelling. Values were set at 0.1–0.3° for the low aggradation angle models, 0.5–0.8° for the mid-range models and 1.0–1.4° for the steeply aggradational models (Fig. 9).

In order to maintain a consistent shoreline trajectory at the large, parasequence-set scale (i.e. whole reservoir), it was necessary to define an additional parameter termed 'offset'. The

long-term shoreline trajectory results from the combined effects of the short-term, parasequence-scale trajectory and the amount of landward dislocation of the shoreline facies tracts associated with the flooding surfaces that bound each of the zones (Fig. 9). A near-constant long-term trajectory was maintained by varying the offset factor between the different aggradation angles (Table 3). The table highlights the target offset and also the achieved, posterior parameters recorded from the actual models. These are reported as P10, P50 and P90 values to illustrate the nature of the distribution. These values for offset are consistent with values documented from outcrop sections (Table 1).

*Barrier coverage* Cemented and shale-covered barriers are common in shoreface and deltaic systems, both associated with parasequence boundaries and bedset-scale clinoforms (O'Byrne & Flint 1995; Taylor *et al.* 1995, 2000; Molenaar *et al.* 1988; Molenaar 1990; Molenaar & Martinus 1990). There is very little quantitative data within the published literature on the degree of barrier coverage and the shape of the cemented bodies. For the purpose of SAIGUP, three levels of barrier coverage were modelled for all of the SAIGUP models (10%, 50% and 90% coverage), with a smaller subset of 12 models having 100% coverage. All levels of coverage were subsequently slightly

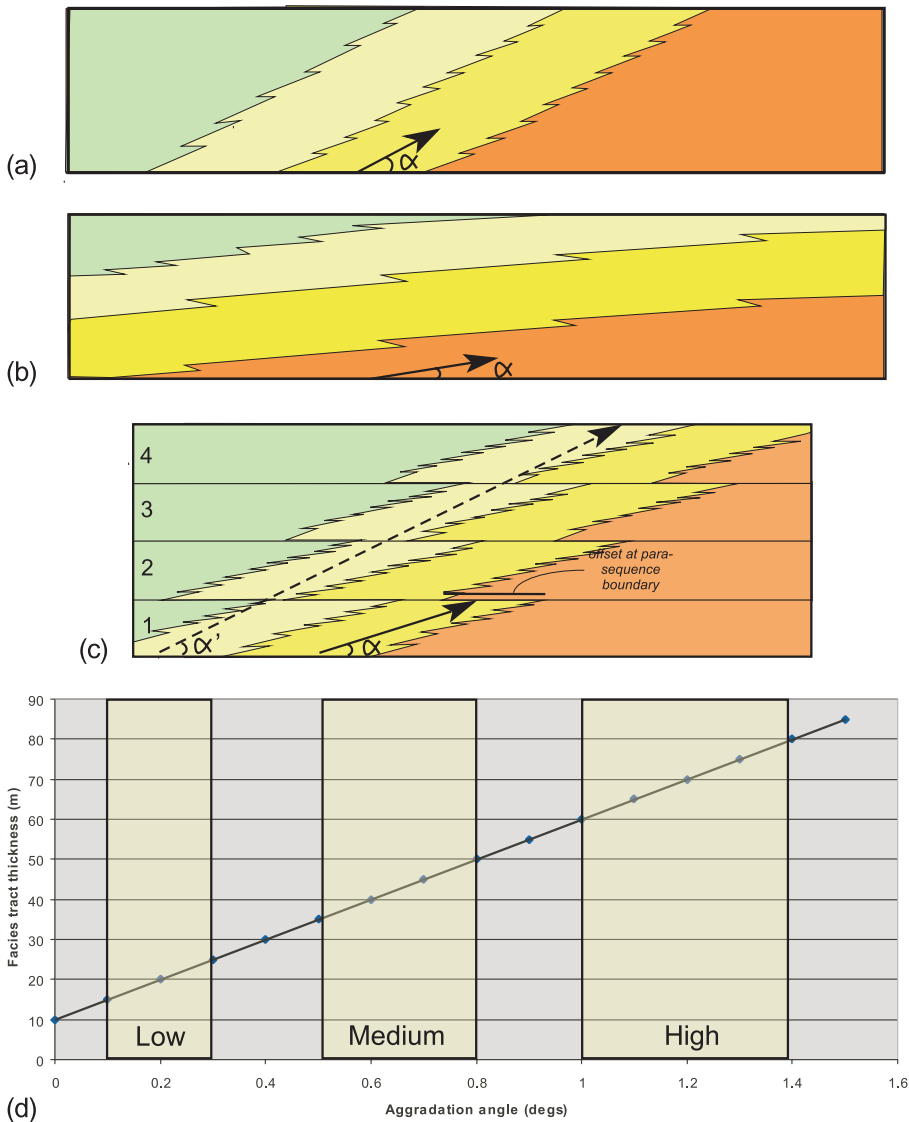


**Fig. 9.** Shoreline trajectory (aggradation angle). (a) System with a high, positive shoreline trajectory and the thick, laterally restricted facies belts. (b) System with a low positive shoreline trajectory and the thinner and more laterally extensive facies belts. (c) Shoreline trajectory in a parasequence set and the occurrence of two trajectories, one for the individual parasequences and one for the parasequence set. Diagram also illustrates the offset associated with the flooding at each parasequence boundary. (d) Graph showing calculated facies tract thickness vs. shoreline trajectory, highlighting the fact that as the trajectory increases so does the thickness of the individual facies belts.

modified by removing the barriers where the fluvial channel deposits were present, since clinoforms are a feature of the delta front and not formed within a channel setting. The resultant channel-controlled connections between otherwise clinoform-bounded upper shoreface compartments have proven extremely important for production from the model containing highly cemented clinoforms (Skorstad *et al.* 2008).

**Progradation direction** The final factor varied during the sedimentological modelling was the progradation- or depositional-dip direction (i.e. the direction in which the shoreline built out). For each set of model parameters described above, three models were built: up, down and across the dominant structural dip. The progradation direction is important because the structural

dip controls the well positions and the waterflood direction during production. Consequently, this parameter records whether the subsequent waterflood will be, up-depositional dip, down-depositional dip or across it (Manzocchi *et al.* 2008). This link between sedimentology and structure does not imply that the structures were active during deposition; the faults are modelled as post-depositional with no related changes in facies thickness or shoreline orientations.

#### Parameters characterized from the real world but kept constant in the models

The above listed parameters were systematically varied within the SAIGUP models to produce the variety of heterogeneity for the study. A number of other parameters were also recorded from the analogue datasets. These are outlined below and their inclusion in the final models is discussed.

**Grain size** The majority of shallow-marine systems have a broadly bimodal grain-size distribution, including a mud fraction which is deposited predominantly in the offshore and to a lesser extent in the coastal plain, and a coarser-grade fraction that makes up the shoreface or delta front. The proportion of mud in the system and the mean grain size of the coarser fraction are key controls on the overall geometry of the system

**Table 3.** Average offset factors between individual parasequences

Model set	Target offset (m)	Achieved offset		
		P10 of distribution	P50 of distribution	P90 of distribution
Low aggradation angle	4406	2400	4123	6000
Moderate aggradation angle	898	510	915	1300
High aggradation angle	289	120	291	420

**Table 4.** Facies tract thickness ranges used in this study

USF and foreshore/UDF (m)	5.0–8.0
LSF/LDF (m)	12.5–17.5
OTZ/prodelta (m)	17.5–22.5
Channel widths (m)	Mean 500, SD 100
Channel thicknesses (m)	Mean 10, SD 2

LDF, lower delta front; LSF, lower shoreface; OTZ, offshore transition zone; SD, standard deviation; UDF, upper delta front; USF, upper shoreface

(Orton & Reading 1993) and affect clinoform dip (Fig. 6), delta area (Fig. 6), percentage of the coastal plain that is emergent and, to a lesser extent, the ultimate shape of the shoreline (Orton & Reading 1993). The majority of the world's siliciclastic shallow-marine reservoirs are sandstones and, for the purpose of SAIGUP, it was decided to keep this parameter constant so that the sand-grade fraction has a modal distribution of fine sand. All other parameters are conditioned accordingly.

**Clinoform dip angle** Clinoforms are seaward-dipping surfaces that represent the position of the depositional profile at one time. They represent boundaries between depositional events and are often mud draped or cemented. Clinoform dip was recorded directly from outcrops of ancient systems (e.g. Fig. 8) and from bathymetric data from modern systems (Table 2). As discussed above, the clinoforms in SAIGUP were modelled as dipping transmissibility barriers that provide barriers or baffles to both horizontal and vertical flow. Within nature, the dip of the clinoforms is a function of the mean grain size of the depositional system, with the dip angle increasing with the grain size (Fig. 6). The dominant depositional processes (i.e. fluvial vs. wave) also affect the clinoform angle, with wave-dominated systems having lower dip angles than fluvial-dominated systems of an equivalent grain size (Tables 1, 2). As shale-draped clinoforms were modelled only in the lobate and elongate shoreline models, a typical value of  $0.5^\circ$  was used as being characteristic of a deltaic system comprised of fine sand (Fig. 6).

**Zone thickness** For the main suite of models, the 80 m section in the SAIGUP field was subdivided into four equally thick zones. Each zone was comprised of one parasequence or shoreline body (see above). The 20 m thickness for each shoreline body is taken from the typical thickness of parasequences commonly described in the literature (Van Wagoner *et al.* 1990; O'Byrne & Flint 1995; Howell & Flint 2004). A series of 24 models were also built with two thicker, 40 m zones and another 24 models with six thinner (16.7 m) zones. The facies tract thicknesses remained constant for these additional models.

**Facies tract thickness** The thickness of the various facies tracts within the individual zones is conditioned directly from observations of ancient systems (Fig. 6). There is a strong link between aggradation angle and subsequent facies tract thickness (Fig. 9d). The significance of this was not appreciated fully at the time the models were built. This relationship and the implications for reservoir geometries will be discussed in greater detail later in the paper. Within the models the values used are drawn from the ranges in Table 4.

The thicknesses of the offshore and the coastal plain were unlimited within the zones, i.e. the coastal plain deposits were used to occupy the area of the zone above and landward of the USF or UDF. Similarly, offshore facies were used to fill the part of the parasequence that lay below and seaward of the OTZ/prodelta. Channel widths and thicknesses within the coastal plain were taken from values typical for the lower delta plain, from the compilation of Reynolds (1999).

**Interfingering factor** In the rock record the degree of shoreline sinuosity controls the degree to which the various facies belts interfinger with one another. The input was measured from the sinuosity of the shorelines in the modern systems. Sinuosity is defined as the ratio between a smoothed profile and the actual shoreline at the observed map scale. The observed mean ratio of 1.7 was then compared to plan views of various RMS models. From this an appropriate RMS parameter value of 1 was selected. No significant difference was observed or modelled between the different shoreline systems (Table 2).

**Delta lobe avoidance factors** Within nature delta lobes create positive topographic features on the seafloor and subsequent lobes will gravitate towards low points and avoid the previous lobes. This is simulated in the equi-thick zones of the SAIGUP model by adding a repulsion factor so that younger lobes avoid the apex of the earlier lobes (if node of lobe 1 is  $X$ , node of lobe 2 is  $X \pm >250$  m). This prevents unrealistic vertical stacking and is especially important where the long axis of the models is perpendicular to the depositional dip.

## MODEL BUILDING PROCEDURE

An automated workflow was developed for building the required sedimentological models, conditioned to the data that had been collected. Models were built within a regular grid in two stages. A 1.5 million cell geomodel was built with a grid cell resolution of  $37.5 \times 37.5 \times 1$  m and this was upscaled to a 96 000 cell simulation model with a resolution of  $75 \times 75 \times 4$  m. Population of the grids was achieved by modelling the facies and then using the facies to control the distribution of petrophysical properties. The models were built in the following, semi-automated stages: (1) drawing input data from database; (2) facies modelling; (3) petrophysical modelling; (4) upscaling and the inclusion of the barriers (clinoform shales and parasequence boundaries). These stages are described in detail below and illustrated in Figures 10 and 11.

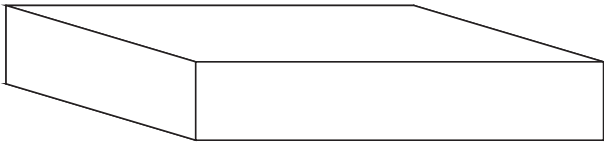
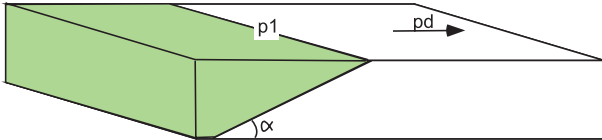
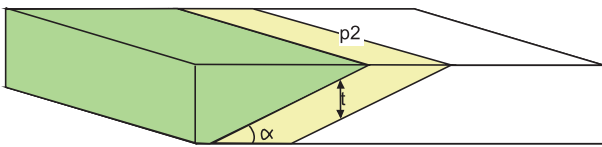
### Drawing input parameters

The facies modelling tools used to build the models include a truncated Gaussian simulation to model the shoreface and delta-front deposits (Facies: Belts in RMS, see MacDonald & Aasen (1994) for a full description); an object-based system to create channels (Facies: Channels in RMS, see Holden *et al.* 1998). To run these models a series of input parameters are required. For the facies: belts modelling these parameters include: (1) the aggradation angle; (2) the shoreline shape; (3) the plan view widths of the facies tracts; (4) the positions of the facies boundaries; (5) the interfingering factor; and (6) the progradation direction. Parameters for the channel modelling delta top include channel proportions, orientation width and thickness and sinuosity. All of these input parameters were taken from the values described above. Within the workflow an IPL script (IPL is RMS's internal programming language) was written to take sets of values from the database and perform the facies modelling automatically. Values were drawn uniformly within the designated ranges defined for the suite of models. All drawn parameters were stored for statistical analysis and model QC.

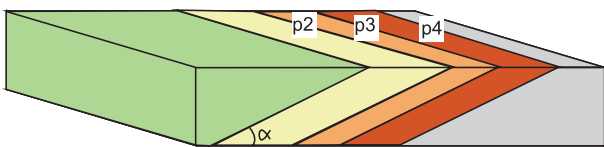
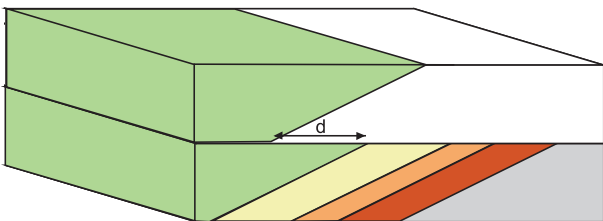
### Facies modelling

All of the facies, except the fluvial channels in the coastal plain, were modelled with the Facies: Belts module in RMS. Facies: Belts uses a truncated Gaussian field algorithm which creates an interfingering transition from a planar contact between two

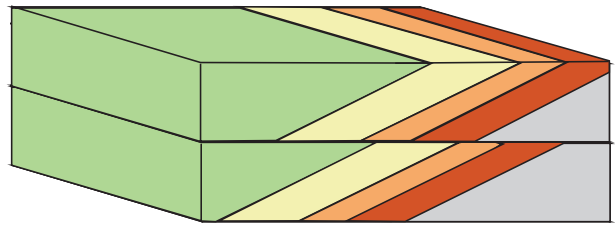
Stage 1. Simulation box for first zone

Stage 2. First facies boundary modelled. Inputs are the plan view position ( $p_1$ ), the progradation direction ( $pd$ ) and the aggradation angle ( $\alpha$ )Stage 3. Subsequent facies boundary modelled. Inputs are the facies tract thickness ( $t$ ) and aggradation angle ( $\alpha$ ) which are used to determine the position of the second facies boundary ( $p_2$ )

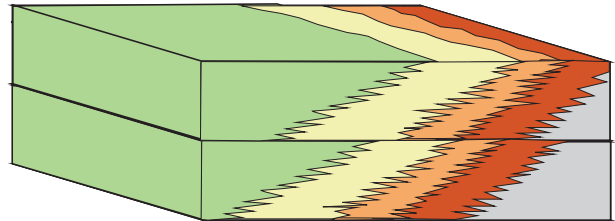
Stage 4. Procedure repeated for the remaining facies in the zone.

Stage 5. The first facies tract position in the overlying zone is determined by the offset ( $d$ ).

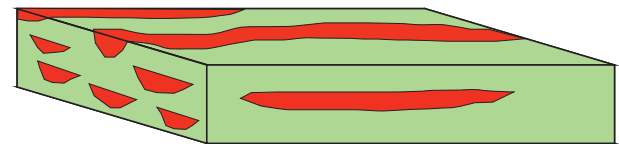
Stage 6. Subsequent facies added as previously.



Stage 7. Truncated Gaussian simulations run to introduce interfingering between belts. Input is the interfingering factor



Stage 8. Fluvial systems modelled in separate simulation box. Input factors are channel width, thickness, proportion, sinuosity and orientation. Repeated for each zone



Stage 9. Channels from stage 8 are merged in to the coastal plain of the final geomodel

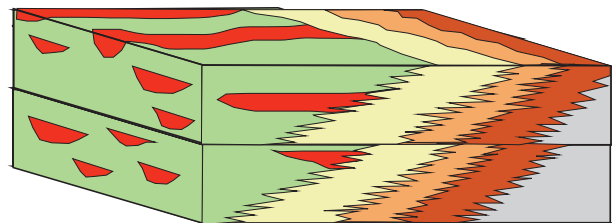


**Fig. 10.** Schematic figure showing the stages involved in the automated building of a single SAIGUP model.

facies (MacDonald & Aasen 1994). This facies modelling algorithm is ideal for reproducing shoreface and deltaic systems where progradation (or retrogradation) of facies that lie adjacent to one another in plan view results in interfingering belts in 3D. The first stage of the facies modelling was to select the plan view positions for the mean boundaries between the five main facies (Fig. 10). Once the position of the first boundary was selected the others were calculated using the desired facies tract thickness and the aggradation angle (Fig. 10). The position of the facies boundaries in the subsequent zones was calculated using an updip offset for the first boundary, designed to simulate the facies dislocation associated with a parasequence-bounding flooding surface. The position of the remaining boundaries within the second zone were again calculated using trigonometry. This procedure continued until the position of all of the boundaries in all of the zones was determined. Once the boundaries were in place the interfingering factor was input and the facies modelling algorithm was run.

As described above, three sets of models were built to represent shorefaces, wave-dominated deltas and river-dominated deltas, with increasing shoreline curvature. In the curved shorelines of the wave-dominated deltas the updip offset between zones was also supplemented by a lateral offset of the focus point, equivalent to the position of the main fluvial input position in the delta. This lateral offset simulated the topographic avoidance associated with delta lobe avulsion (see above). In the highly elongate shorelines of the river-dominated deltas, two delta lobes were included in each zone. This was achieved by building two separate realizations of each zone, using an avoidance factor to separate the lobes. The realizations were then merged so that any grid cell was assigned the most proximal facies from either of the two realizations.

The channels in the coastal plain were modelled using the Facies: Channels module in RMS. The channels for a specific zone were built within a separate realization of that zone and then merged into the coastal plain facies in a subsequent merge operation (Fig. 10). The sinuosity, width and thickness of the

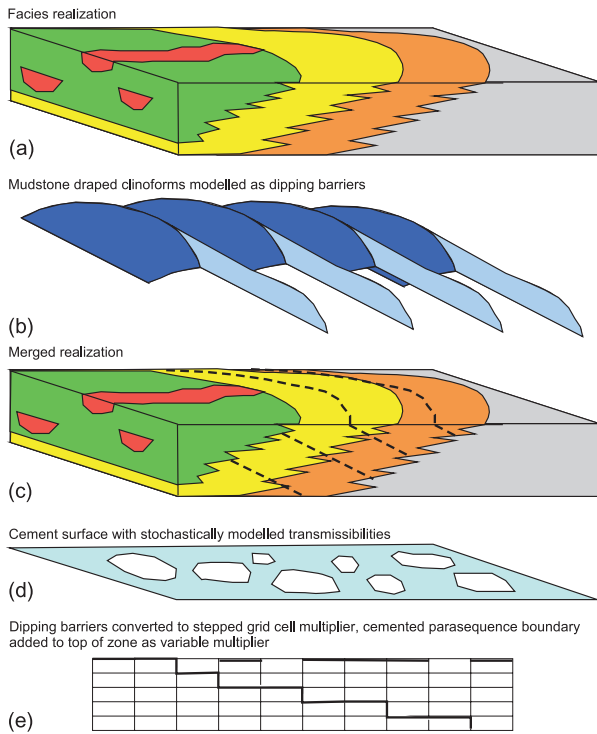


**Fig. 11.** Schematic figure to show the method for adding cemented horizons and dipping barriers in the SAIGUP models.

channels was drawn from a constant range as described above, while the proportion of the channels was dependent on the shoreline type. The mean channel orientation was set perpendicular to the shoreline orientation in the shoreface models. Channels in the deltas were modelled with a radial, fan-shaped distribution, conditioned on the focus point within the facies belts realization.

### Petrophysics and upscaling

The distribution of the petrophysical parameters is controlled by the facies. Porosity ( $POR$ ), clay content ( $V_{shale}$ ) and vertical ( $K_v$ ) and horizontal ( $K_h$ ) permeability for the low permeability facies (offshore, offshore transition and coastal plain), and log-permeability for the high permeability facies (channel, upper shoreface, lower shoreface) are modelled as correlated Gaussian fields (Haldorsen & Damsleth 1990) with different distributions within the different facies (Table 5).

Correlations (0.8) were defined between each of the following four stochastic petrophysical properties: porosity,  $K_h$ ,  $K_v$ ,  $V_{shale}$  (Skorstad *et al.* 2005). Variograms used to control the lateral and vertical distribution of the petrophysical properties are summarized in Table 6. To investigate the effects of variogram orientation, these were rotated through  $90^\circ$  for a

subset of the models (Skorstad *et al.* 2005). This resulted in a subset of models with identical facies distributions and two petrophysical representations.

Differences in small-scale sedimentological structure and properties were included in the grid-block relative permeability functions (Stephen *et al.* 2008). Upscaling from the geo-grid to the simulation grid was achieved using a flow-based upscaling approach similar to the Warren *et al.* (1961) method but with a linear pressure fall rather than no flow at the boundaries. This choice of method is not overly sensitive to local areas with zero permeability such as the non-reservoir, coastal plain, offshore transition zone and offshore facies associations, where no-flow conditions would produce many cells with zero permeability.

### Barriers at clinoforms and parasequence boundaries

Two types of barrier were placed in the SAIGUP models. Parasequence boundaries provide baffles and barriers to vertical flow, while the shales associated with the clinoform surfaces impede both vertical and horizontal flow. The parasequence boundaries were modelled as transmissibility multipliers on the zone boundaries.

The clinoform barriers were modelled as dipping, staircase, transmissibility multipliers (Fig. 11). The position of the multipliers was achieved by creating an elliptic cone-shaped surface that followed the plan-view shoreline shape of the facies and dipped in a seaward direction (Fig. 11). The surface had a variable transmissibility multiplier field. The cone was projected into the simulation grid and placed as a multiplier on cells that contained upper shoreface, lower shoreface and offshore transition zone facies. The clinoforms were not included in the offshore facies, because the permeability was already effectively zero. They were not included in the coastal plain- or fluvial channel facies because in the real world they are a feature of the delta front and do not occur landward of the shoreline.

Sealing on both the parasequence and the clinoform barriers varied spatially from open (transmissibility multipliers of one) to closed (multipliers of zero). A transformed Gaussian field was used to model the multipliers so that individual cell boundaries have a strong correlation with their neighbours and a gradual transition from complete sealing to non-sealing was obtained. The parameters were set to achieve three levels of average sealing across the surfaces (10%, 50% and 90%). The clinoforms were modelled with slight repulsion in order to prevent clustering and the clinoform frequency was controlled by the shoreline type. Barriers between the parasequence boundaries were included in all the models. Mud-draped clinoforms were not included in the straight shoreline (shoreface) systems, there were 1–3 per zone in the wave-dominated deltas and between 4 and 9 in each lobe (total of up to 18 per zone) in the river-dominated delta systems.

**Table 5.** Petrophysical parameters assigned to facies

Facies	Log ( $K_v$ )		$K_v$ Exp	Log ( $K_h$ )		$K_h$ Exp	POR		$V_{shale}$	
	Exp	Std		Exp	Std		Exp	Std	Exp	Std
CH	4	1	90.02	5.6	1	445.9	0.2	0.04	0.2	0.04
CP	NA	NA	0.0	-1	2	2.72	0.05	0.01	0.5	0.1
USF	4.6	1	164.0	6.25	1	854.1	0.2	0.02	0.15	0.03
LSF	0	1	1.65	4	1	90.02	0.15	0.02	0.25	0.05
OTZ	NA	NA	0.0	2.5	1	20.09	0.12	0.02	0.4	0.08
OFF	NA	NA	0.0	-3	0.5	0.06	0.02	0.01	0.6	0.12

CH, channel; CP, coastal plain; LSF, lower shoreface; OFF, offshore; OTZ, offshore transition zone; USF, upper shoreface

**Table 6.** Variogram details for petrophysical modelling

Parameter	CP	CH	USF	LSF	OTZ	OFF
Range main direction	1000	800	2000	4000	4000	2000
Range normal direction	1000	250	1000	2000	2000	1000
Range, vertical	6	10	8	4	2	1
Azimuth direction	0	0	90	90	90	90

Ranges in metres. See Table 5 for abbreviations

### MODEL QC AND LIMITATIONS

A set of 408 sedimentological models were retained. These capture a range of heterogeneities that exist within progradational shallow-marine reservoirs. It is important to note that none of these models represents a direct, deterministic representation of any specific modern or ancient system. Rather the models are designed to capture the character and range of variability that could potentially exist. It is possible that values for some of the variables could exceed those used in the modelling and other combinations of the variables may occur. It is also possible that in specific systems other variables, beyond those modelled, may be important controlling factors on reservoir geometry and performance.

As the modelling procedure was automated it was important that the models were quality controlled by a geologist. The principal quality control method was to simply visually inspect the models and determine if they were geologically realistic. Facies belt geometries in cross-section and plan view were checked, as were facies juxtapositions. Models were also compared qualitatively to modern and ancient systems that occupied comparable SAIGUP parameter space. In virtually all cases, a good match was observed.

The models contain a number of limitations, many of which stem from the need to capture a very wide and highly variable parameter space or from the need for automated modelling. The following limitations exist within the models.

- 1. The use of parallel-sided zones.** In the real world the top of a parasequence is flat in the coastal plain, dips seaward parallel to the old shoreface or delta front and is close to flat, dipping very gently seaward in the offshore. This topography is inherited by the subsequent parasequence and provides additional accommodation which affects the facies tract thicknesses. The use of parallel-sided zones produces some minor geometric problems related to aggradation angles and facies tract thickness. Sensitivity studies, which include the modelling of real-world outcrops from the Spring Canyon and Desert Members of the Blackhawk Formation, Utah (Liv Johanssen, pers. comm.), indicate that this does not make a significant difference to the final flow results.
- 2. The use of equi-thick zones in all of the models.** In the real world there is a clear link between zone thickness and aggradation angle, with higher aggradation angles resulting in thicker zones. This problem was overcome somewhat by using two aggradation angles (one for the zone and one for the model – see above) and having a smaller offset factor used in the models with higher zone aggradation angles. A subset of models with thicker zones was also generated and, although it would be possible to compare these to the appropriate 20 m thick zone model, this has yet to be done.
- 3. Using only one set of facies tract thicknesses for all of the models.** There is a demonstrable link between facies tract thickness and aggradation angle, as discussed above. Increased aggradation angle results in an increase in the thickness of the facies belts. This has not been captured but

could be addressed with further work; this is beyond the scope of the present study.

Despite these limitations, it is believed that the 408 models adequately capture a range of heterogeneities that exist within progradational, fluvial- to wave-dominated shallow-marine systems. These models form the basis for the various production sensitivity modelling studies performed within the SAIGUP project. These studies are summarized by Manococchi *et al.* (2008).

### CONCLUSIONS

The four key components of heterogeneity within clastic shallow-marine systems were defined as (1) the degree of fluvial influence at the shoreline; (2) the aggradation angle; (3) the presence of cemented and shale-covered barriers; and (4) the progradation direction. The degree of fluvial influence controls the shape of the shoreline, the proportion of channels and the abundance of shale-draped clinoform surfaces. The aggradation angle controls the vertical and lateral stacking of the facies. A suite of 408 models were built to attempt to capture the variability that exists within real-world reservoirs of this nature.

To populate the models, data were collected from 51 modern and ancient systems. These data quantify the range of variability that exists within progradational shallow-marine systems, both within the individual parameters and the degree of parameter interdependency. Models were built using Roxar's RMS software. An automated modelling procedure was developed, which sampled input parameters from the database and produced the models in a series of steps. Visual comparisons between the synthetic SAIGUP models and images of modern shoreline systems provided a useful quality control of the models. The results are favourable and indicate that the values used to condition the SAIGUP models produce realistic models.

This paper has benefited from constructive reviews by Gary Hampson, Allard Martinius and John Walsh. The European Commission Framework 5 Hydrocarbons Reservoir Programme is thanked for partly funding SAIGUP. Other members of the SAIGUP project not included in the authorship of this paper are acknowledged and thanked sincerely for ongoing discussion and input. Industrial partners, Shell, BG and Badley Geoscience, are also acknowledged for access to data. We are very grateful to Badley Geoscience, BG International, Roxar and Shell for their support of the SAIGUP project and for their sponsorship of the production of this thematic set.

### REFERENCES

- Abbotts, F.V. & van Kuyk, A.D. 1997. Using 3D geological modelling and connectivity analysis to locate remaining oil in the Brent reservoir of the mature Brent Field. *Society for Petroleum Engineers*, **38473**, 107–114.
- Ainsworth, R.B. 2005. Sequence stratigraphic-based analysis of reservoir connectivity: influence of depositional architecture – a case study from a marginal marine depositional setting. *Petroleum Geoscience*, **11**, 257–276.
- Ainsworth, R.B., Sanlung, M. & Duivenvoorden, S.T.C. 1999. Correlation Techniques, Perforation Strategies and Recovery Factors. An Integrated 3-D Reservoir Modeling Study, Sirikit Field, Thailand. *American Association of Petroleum Geologists Bulletin*, **83**, 1535–1551.
- Ainsworth, R.B., Flint, S.S. & Howell, J. 2008. Predicting Coastal Depositional Style: Influence of Basin Morphology and Accommodation/Sediment Supply Regime within a Sequence Stratigraphic Framework. In: Hampson, G.J., Steel, R., Burgess, P. & Dalrymple, R. (eds) *Recent Advances in Shallow-marine Stratigraphy*. Society of Economic Paleontologists and Mineralogists, Special Publication (in press).
- Anderson, P.B., Chidsey, T.C. Jr, Ryer, T.A., Adams, R.D. & McClure, K. 2004. Geologic Framework, Facies, Paleogeography, and Reservoir Analogs of the Ferron Sandstone in the Ivie Creek Area, East-Central Utah. In: Chidsey, T.C. Jr, Adams, R.D. & Morris, T.H. (eds) *Regional to Wellbore Analog for Fluvial-Deltaic Reservoir Modeling: The Ferron Sandstone of*

- Utah. American Association of Petroleum Geologists, Studies in Geology, **50**, 331–356.
- Back, S., Tioe, H.J., Thang, T.X. & Morley, C.K. 2005. Stratigraphic development of synkinematic deposits in a large growth-fault system, onshore Brunei Darussalam. *Journal of the Geological Society, London*, **162**, 243–257.
- Bhattacharya, J.P. & Giosan, L. 2003. Wave-influenced deltas: geomorphological implications for facies reconstruction. *Sedimentology*, **50**, 187–210.
- Bhattacharya, J.P. & Tye, R.S. 2004. Searching for Modern Ferron Analogs and Application to Subsurface Interpretation. In: Chidsey, T.C. Jr, Adams, R.D. & Morris, T.H. (eds) *Regional to Wellbore Analog for Fluvial-Deltaic Reservoir Modeling: The Ferron Sandstone of Utah*. American Association of Petroleum Geologists, Studies in Geology, **50**, 39–57.
- Bhattacharya, J.P. & Walker, R.G. 1992. Deltas. In: Walker, R.G. & James, N.P. (eds) *Facies models: response to sea-level change*. Geological Association of Canada, 157–177.
- Boyd, R., Dalrymple, R.W. & Zaitlin, B.A. 1992. Classification of clastic coastal depositional environments. *Sedimentary Geology*, **80**, 139–150.
- Chidsey, T.C. Jr, Adams, R.D. & Morris, T.H. (eds) 2004. *Regional to Wellbore Analog for Fluvial-Deltaic Reservoir Modeling: The Ferron Sandstone of Utah*. American Association of Petroleum Geologists Studies in Geology, **50**.
- Coleman, J.M. & Prior, D.B. 1982. Deltas environments and facies. In: Scholle, P.A. & Pearing, D. (eds) *Sandstone Depositional Environments*. American Association of Petroleum Geologists Memoir, **31**, 139–178.
- Curry, J.R., Emmel, F.J. & Crampton, P.J.S. 1969. Holocene history of a strand plain, lagoonal coast, Nayarit, Mexico. In: Castaneres, A.A. & Phleger, F.B. (eds) *Coastal Lagoons. A Symposium*. Universidad Nacional Autónoma, Mexico, 63–100.
- Dalrymple, R.W., Baker, E.K., Harris, P.T. & Hughes, M. 2003. Sedimentology and stratigraphy of a tide-dominated, foreland-basin delta (Fly River, Papua New Guinea). In: Sidi, F.H., Nummedal, D., Imbert, P., Darman, H. & Posamentier, H.W. (eds) *Tropical Deltas of Southeast Asia – Sedimentology, Stratigraphy, and Petroleum Geology*. Society of Economic Paleontologists and Mineralogists Special Publication, **76**, 147–173.
- Dominguez, J.M.L. 1996. The São Francisco strandplain: a paradigm for wave-dominated deltas? In: De Batist, M. & Jacobs, P. (eds) *Geology of siliciclastic shelf seas*. Geological Society, London, Special Publications, **117**, 217–231.
- Dominguez, J.M.L., Martin, M. & Bittencourt, A. 1987. Sea-level history and Quaternary evolution of river mouth-associated beach-ridge plains along the East-Southeast Brazilian coast; a summary. In: Nummedal, D., Pilkey, O.H. & Howard, J.D. (eds) *Sea-level fluctuation and coastal evolution*. Society of Economic Paleontologists and Mineralogists, Special Publication, **41**, 115–125.
- Doust, H. & Omatsola, E. 1990. Niger Delta. In: Edwards, J.D. & Santogrossi, P.A. (eds) *Divergent/Passive margin basins*. American Association of Petroleum Geologists Memoir, **48**, 201–238.
- Driscoll, N.W. & Karner, G.D. 1999. Three-dimensional quantitative modeling of clinoform development. *Marine Geology*, **154**, 383–398.
- Fitzsimmons, R. & Johnson, S. 2000. Forced regressions; recognition, architecture and genesis in the Campanian of the Bighorn Basin, Wyoming. In: Hunt, D. & Tucker, M.E. (eds) *Sedimentary Responses to Forced Regressions*. Geological Society, London, Special Publications, **174**, 113–139.
- Galloway, W.E. 1975. Process Framework for describing the morphological and stratigraphic evolution of deltaic depositional systems. In: Broussard, M.L. (ed.) *Deltas, models for exploration*. Houston Geological Society, 87–98.
- Google Earth. 2007. World Wide Web address: <http://www.earth.google.com>.
- Haldorsen, H.H. & Damsleth, E. 1990. Stochastic modelling. *Journal of Petroleum Technology*, **42**, 404–412.
- Hampson, G.J. 2000. Discontinuity surfaces, clinoforms and facies architecture in a wave-dominated, shoreface-shelf parasequence. *Journal of Sedimentary Research*, **70**, 325–340.
- Hampson, G.J. & Howell, J.A. 2005. Sedimentologic and geomorphic characterization of ancient wave-dominated deltaic shorelines; Upper Cretaceous Blackhawk Formation, Book Cliffs, Utah, USA. In: Giosan, L. & Bhattacharya, J.P. (eds) *River Deltas – Concepts, Models and Examples*. Society for Economic Paleontologists and Mineralogists Special Publication, **83**, 133–154.
- Hampson, G.J. & Storms, J.E.A. 2003. Geomorphological and sequence variability in wave dominated, shoreface-shelf parasequences. *Sedimentology*, **50**, 667–701.
- Hampson, G.J., Sixsmith, P.J. & Johnson, H.D. 2004. A sedimentological approach to refining reservoir architecture in a mature hydrocarbon province: the Brent Province, UK North Sea. *Marine and Petroleum Geology*, **21**, 457–484.
- Helland-Hansen, W., Badley, M.E., Lomo, L. & Steel, R.J. 1992. Advance and retreat of the Brent Delta: recent contributions to the depositional model. In: Morton, A.C., Haszeldine, R.S., Giles, M.R. & Brown, S. (eds) *Geology of the Brent Group*. Geological Society, London, Special Publications, **61**, 109–127.
- Helland-Hansen, W. & Martinsen, O.J. 1996. Shoreline trajectories and sequences: description of variable depositional-dip scenarios. *Journal of Sedimentary Research*, **66**, 670–688.
- Hodgetts, D., Imber, J., Childs, C., Flint, S., Howell, J., Kavanagh, J., Nell, P. & Walsh, J. 2001. Sequence stratigraphic responses to shoreline-perpendicular growth faulting in shallow marine reservoirs of the Champion Field, offshore Brunei Darussalam, South China Sea. *American Association of Petroleum Geologists Bulletin*, **85**, 433–457.
- Holden, L., Hauge, R., Skare, O. & Skorstad, A. 1998. Modeling of fluvial reservoirs with object models. *Mathematical Geology*, **30**, 473–496.
- Howell, J. 2005. Sedimentary environments; shoreline and shoreface deposits. *Encyclopedia of geology*, **4**. Elsevier Academic Press, 570–580.
- Howell, J. & Flint, S. 2004. Sequences and systems tracts in the Book Cliffs. In: Coe, A. (ed.) *The sedimentary record of sea-level change*. Cambridge University Press, Cambridge, 135–208.
- Howell, J.A., Flint, S.S. & Hunt, C. 1996. Sedimentological aspects of the Humber Group (Upper Jurassic) of the South Central Graben, UK North Sea. *Sedimentology*, **43**, 89–114.
- Howell, J.A., Vassel, A. & Aune, T. 2008. Modelling of dipping clinoform barriers within lowstand and highstand deltas: A comparative outcrop study from the Cretaceous Western Interior Basin USA. In: Griffiths, P., Price, S., Hegre, J. & Robinson, A. (eds) *The Future of Geological Modelling in Hydrocarbon Development*. Geological Society, London, Special Publications, (in press).
- Jennette, D.C. & Riley, C.O. 1996. Influence of relative sea level on facies and reservoir geometry of the Middle Jurassic lower Brent Group, UK North Viking Graben. In: Howell, J.A. & Aitken, J.F. (eds) *High Resolution Sequence Stratigraphy: innovations and applications*. Geological Society, London, Special Publications, **104**, 87–113.
- Johnson, H.D., Mackay, T.A. & Stewart, D.J. 1986. The Fulmar oil-field (central North Sea); geological aspects of its discovery, appraisal and development. *Marine and Petroleum Geology*, **3**, 99–125.
- Kamola, D.L. & Huntoon, J.E. 1995. Repetitive stratal patterns in a foreland basin sandstone and their possible tectonic significance. *Geology*, **23**, 177–180.
- Keogh, K., Rippon, J., Hodgetts, D., Howell, J. & Flint, S. 2005. Improved understanding of fluvial architecture using 3-D geological models: A case study of the Westphalian A Silkstone Rock, Pennine Basin, U.K. In: Blum, M. (ed.) *Proceedings of the 5th International Conference on Fluvial Sedimentology*. International Association of Sedimentologists Special Publication, **35**, 481–491.
- Li, H. & White, C.D. 2003. Geostatistical models for shales in distributary channel point bars (Ferron Sandstone, Utah): From ground-penetrating radar data to three-dimensional flow modeling. *American Association of Petroleum Geologists Bulletin*, **87**, 1851–1868.
- MacDonald, A.C. & Aasen, J.O. 1994. A prototype procedure for stochastic modeling of facies tract distribution in shoreface reservoirs. In: Yarus, J.M. & Chambers, R.L. (eds) *Stochastic modeling and geostatistics; principles, methods, and case studies*. American Association of Petroleum Geologists Computer Applications in Geology, 91–108.
- Manzocchi, T., Carter, J.N., Skorstad, A. et al. 2008. Sensitivity of the impact of geological uncertainty on production from faulted and unfaulted shallow-marine oil reservoirs: objectives and methods. *Petroleum Geoscience*, **14**, 3–15.
- Martinius, A.W., Ringrose, P.S., Broström, C., Elfenbein, C., Naess, A. & Ringås, J.E. 2005. Reservoir Challenges of heterolithic tidal sandstone reservoirs in the Halten Terrace, mid-Norway. *Petroleum Geoscience*, **11**, 3–16.
- Molenaar, N. 1990. Calcite cementation in shallow-marine Eocene sandstones and constraints of early diagenesis. *Journal of the Geological Society, London*, **147**, 759–768.
- Molenaar, N. & Martinius, A.W. 1990. Origin of nodules in mixed siliciclastic-carbonate sandstones, the Lower Eocene Roda Sandstone Member, southern Pyrenees, Spain. *Sedimentary Geology*, **66**, 277–293.
- Molenaar, N., van de Bilt, E.R., van den Hoek, O. & Nio, S.D. 1988. Early diagenetic alternation of shallow-marine mixed sandstones: An example from the Lower Eocene Roda Sandstone Member, Tremp-Graus Basin, Spain. *Sedimentary Geology*, **55**, 295–318.
- Muto, T. & Steel, R.J. 2001. Auto-stepping during the transgressive growth of deltas: results from flume experiments. *Geology*, **29**, 771–774.
- NASA. 2003. Earth Science Enterprise. World Wide Web Address: <https://zulu.ssc.nasa.gov/mrsid/>.
- NASA. 2004. The Earth From Space. World Wide Web Address: <http://eol.jsc.nasa.gov/sseop/efs/>.
- Newman, K.F. & Chan, M.A. 1991. Depositional facies and sequences in the Upper Cretaceous Panther Tongue Member of the Star Point Formation, Wasatch Plateau, Utah. In: Chidsey, T.C. Jr (ed.) *Geology of east-central Utah*, **19**. Utah Geological Association, 65–75.
- O'Byrne, C.J. & Flint, S.S. 1995. Sequence, parasequence and intraparsequence architecture of the Grassy Member, Blackhawk Formation, Book Cliffs, Utah, USA. In: Van Wagoner, J.C. & Bertram, G.T. (eds) *Sequence Stratigraphy of Foreland Basin Deposits*. American Association of Petroleum Geologist Memoir, **64**, 225–257.

- Olariu, C. & Bhattacharya, J.P. 2006. Terminal Distributary Channels and Delta Front Architecture of River-Dominated Delta Systems. *Journal of Sedimentary Research*, **76**, 212–233.
- Orton, G.J. & Reading, H.G. 1993. Variability of deltaic processes in terms of sediment supply, with particular emphasis on grain size. *Sedimentology*, **40**, 475–512.
- Pattison, S.A.J. 1995. Sequence stratigraphic significance of sharp-based lowstand shoreface deposits, Kenilworth Member, Book Cliffs, Utah. *American Association of Petroleum Geologists Bulletin*, **79**, 444–462.
- Pattison, S.A.J. 2005. Isolated highstand shelf sandstone body of turbiditic origin, lower Kenilworth Member, Cretaceous Western Interior, Book Cliffs, Utah, USA. *Sedimentary Geology*, **177**, 131–144.
- Reading, H.G. & Collinson, J.D. 1996. Clastic Coasts. In: Reading, H.G. (ed.) *Sedimentary Environments: process, facies and stratigraphy*. Blackwells, UK, 184–231.
- Reynolds, A.D. 1999. Dimensions of paralic sandstone bodies. *American Association of Petroleum Geologists Bulletin*, **83**, 211–229.
- Ryer, T.A. 1981. Deltaic coals of Ferron Sandstone Member of Mancos Shale; predictive model for Cretaceous coal-bearing strata of Western Interior. *American Association of Petroleum Geologists Bulletin*, **65**, 2323–2340.
- Ryer, T.A. & Anderson, P.B. 2004. Facies of the Ferron Sandstone, East-Central Utah. In: Chidsey, T.C. Jr, Adams, R.D. & Morris, T.H. (eds) *Regional to Wellbore Analog for Fluvial-Deltaic Reservoir Modeling: The Ferron Sandstone of Utah*. American Association of Petroleum Geologists, Studies in Geology, **50**, 59–78.
- Sandal, S.T. (ed.) 1996. *The Geology and Hydrocarbon Resources of Negara Brunei Darussalam*. Syabas, Bandar Seri Begawan.
- Sestini, G. 1989. Nile Delta: a review of depositional environments and geological history. In: Whateley, M.K.G. & Pickering, K.T. (eds) *Deltas: Sites and Traps for Fossil Fuels*. Geological Society, London, Special Publications, **41**, 99–127.
- Skorstad, A., Kolbjørnsen, O., Fjellvoll, B., Howell, J., Manzocchi, T. & Carter, J.N. 2005. Sensitivity of oil production to petrophysical heterogeneities. In: Leuangthong, O. & Deutsch, C.V. (eds) *Geostatistics Banff*. Springer, Dordrecht, 723–730.
- Skorstad, A., Kolbjørnsen, O., Manzocchi, T., Carter, J.N. & Howell, J.A. 2008. Combined effects of structural, stratigraphic and well controls on production variability in faulted shallow-marine reservoirs. *Petroleum Geoscience*, **14**, 45–54.
- Somoza, L., Barnolas, A., Arasa, A., Maestro, A., Rees, J.G. & Hernandez-Molina, F.J. 1998. Architectural stacking patterns of the Ebro delta controlled by Holocene high-frequency eustatic fluctuations, delta-lobe switching and subsidence processes. *Sedimentary Geology*, **117**, 11–32.
- Stephen, K.D., Yang, C., Carter, J.N., Howell, J.A., Manzocchi, T. & Skorstad, A. 2008. Upscaling uncertainty analysis in a shallow-marine environment. *Petroleum Geoscience*, **14**, 71–84.
- Swift, D.J.P., Tillman, R.W., Oertel, G.F. & Thorne, J.A. (eds) 1991. *Shelf sand and sandstone bodies: geometry, facies and sequence stratigraphy*. International Association of Sedimentologists Special Publication, **14**.
- Somme, T.O., Howell, J.A., Hampson, G.J. & Storms, J.E.A. 2008. Genesis architecture and numerical modelling of intra-parasequence discontinuity surfaces in wave-dominated deltaic deposits: Upper Cretaceous Sunnyside Member, Blackhawk Formation, Book Cliffs, Utah, USA. In: Hampson, G.J., Steel, R., Burgess, P. & Dalrymple, R. (eds) *Recent Advances in Shallow-marine Stratigraphy*. Society of Economic Paleontologists and Mineralogists, Special Publication (in press).
- Taylor, K.G., Gawthorpe, R.L. & VanWagoner, J.C. 1995. Stratigraphic control on laterally persistent cementation, Book Cliffs, Utah. *Journal of the Geological Society, London*, **152**, 225–228.
- Taylor, K.G., Gawthorpe, R.L., Curtis, C.D., Marshall, J.D. & Awwiller, D.N. 2000. Carbonate cementation in a sequence-stratigraphic framework: Upper Cretaceous sandstones, Book Cliffs, Utah-Colorado. *Journal of Sedimentary Research*, **70**, 360–372.
- Van Wagoner, J.C., Mitchum, R.M., Campion, K.M. & Rahmanian, V.D. 1990. *Siliclastic sequence stratigraphy in well logs, cores, and outcrops*. American Association of Petroleum Geologists, Methods in Exploration, **7**.
- Van den Bergh, T.C.V. & Garrison, J.R. Jr 2004. The Geometry, Architecture, and Sedimentology of Fluvial and Deltaic Sandstones Within the Upper Ferron Sandstone Last Chance Delta: Implications for Reservoir Modelling. In: Chidsey, T.C. Jr, Adams, R.D. & Morris, T.H. (eds) *Regional to Wellbore Analog for Fluvial-Deltaic Reservoir Modeling: The Ferron Sandstone of Utah*. American Association of Petroleum Geologists, Studies in Geology, **50**, 451–498.
- Walker, R.G. & Plint, A.G. 1992. Wave and storm dominated shallow marine system. In: Walker, R.G. & James, N.P. (eds) *Facies models: response to sea-level change*. Geological Association of Canada, 219–238.
- Warren, J.E., Skiba, F.F. & Price, H.S. 1961. An evaluation of the significance of permeability measurements. *Journal of Petroleum Technology*, **13**, 739–744.
- Whateley, M.K.G. & Pickering, K.T. (eds) 1989. *Deltas: Sites and Traps for Fossil Fuels*. Geological Society, London, Special Publications, **41**.
- Zaitlin, B.A., Dalrymple, R.W. & Boyd, R. 1994. The stratigraphic organization of incised-valley systems associated with relative sea-level change. In: Dalrymple, R., Boyd, R. & Zaitlin, B.A. (eds) *Incised-valley systems; origin and sedimentary sequences*. Society for Sedimentary Geology, Special Publication, **51**, 45–62.